buildings

MDPI

Article

Mechanical Properties, Microstructure, and Water Absorption of Concrete Reinforced with Surface-Treated Basalt Fibers and Nanosilica

Lucas Katerski [1], Janete Eunice Zorzi [2] and Giovani Dambros Telli [1,*]

[1] Área do Conhecimento de Ciências Exatas e Engenharias, Universidade de Caxias do Sul, Rua Francisco Getúlio Vargas, 1130, Caxias do Sul 95070-560, RS, Brazil; lkaterski@ucs.br
[2] Independent Researcher, Farroupilha 95170-444, RS, Brazil; jezorzi@gmail.com
* Correspondence: gdtelli@ucs.br

Abstract

The development of fiber- and nanomaterial-modified cementitious composites has attracted increasing attention for their potential to enhance concrete performance and durability, contributing to more efficient and sustainable construction materials. This study investigated the influence of basalt fiber (BF), fiber surface treatment, and nanosilica (NS) on the mechanical properties, workability, microstructure, and capillary water absorption of concrete. Initially, basalt fiber-reinforced concrete (BFRC) mixtures containing fibers with lengths of 3, 6, and 9 mm at contents of 0.1%, 0.3%, and 0.5% by mass of cement were evaluated. Then, the selected 9 mm basalt fibers were surface-treated with HCl, followed by the incorporation of colloidal nanosilica at 1.5% and 3.0% by mass of cement. Compressive and flexural strengths, capillary water absorption, and scanning electron microscopy (SEM) were evaluated. The results showed that higher fiber contents negatively affected workability and mechanical performance, whereas nanosilica improved the performance of concrete containing treated basalt fibers. The highest compressive and flexural strengths among the investigated mixtures were obtained with 0.3% treated 9 mm basalt fibers combined with 3.0% nanosilica. At 63 days, this mixture reached compressive and flexural strengths of 34.87 and 7.57 MPa, representing an increase of 28.2% and 8.3%, respectively, compared with the reference concrete. The incorporation of 3.0% nanosilica also reduced capillary water absorption, particularly at fiber contents of 0.3% and 0.5%. SEM images suggested a denser cementitious matrix and improved fiber–matrix contact. The combined use of treated basalt fibers and nanosilica improved mechanical and microstructural performance while reducing capillary water absorption.

Keywords: concrete; basalt fiber; nanosilica; mechanical properties; water absorption

Check for updates

Academic Editor: Ahmet Benli

Received: 1 October 2026
Revised: 22 October 2026
Accepted: 3 November 2026
Published: 6 November 2026

Copyright: © 2026 by the authors. Licensee MDPI, Basel, Switzerland. This article is an open access article distributed under the terms and conditions of the Creative Commons Attribution (CC BY) license.

1. Introduction

Concrete offers several advantages, including good workability, durability, and mechanical strength, making it the most widely used construction material [1]. Currently, the construction industry is increasingly focused on developing and adopting sustainable materials and environmentally friendly technologies in response to growing concerns about environmental protection and the need to preserve natural resources [2–4]. Improving the mechanical performance and durability of concrete through material modification represents an important strategy for developing more efficient and durable cementitious composites [5]. Various types of fibers, such as steel, carbon, and glass fibers, have been

incorporated into concrete to enhance its mechanical performance [6]. Their addition aims to improve properties such as flexural strength, fatigue resistance, and flexural toughness, among others [7,8].

The addition of fibers can improve the structural performance of concrete by controlling crack formation and propagation, improving its mechanical properties, including tensile, compressive, and flexural strength [9]. They act by transferring internal stresses across cracks, providing a bridging effect that can improve ductility, post-cracking tensile strength, fatigue resistance, and impact resistance [10,11]. However, the effectiveness of fiber reinforcement depends on the fiber–matrix bond, fiber content, and the characteristics of the interfacial transition zone (ITZ). Different fiber materials and geometries can affect this interaction. Smooth and straight steel fibers may exhibit limited interfacial bonding with the cementitious matrix [12] whereas glass fibers can experience breakage and non-uniform dispersion [13].

Among the different fibers used for concrete reinforcement, basalt fibers have attracted increasing attention due to their favorable mechanical properties and potential application in cementitious composites [14]. Compared with other commonly used fibers, basalt fibers exhibit beneficial mechanical properties, greater durability than glass fibers, and lower cost than carbon fibers, making them an attractive alternative for reinforcing cementitious composites [6,15–17]. Beyond their mechanical performance, basalt fibers offer environmental and economic advantages over conventional reinforcing fibers. Their production requires considerably less energy than that of conventional fibers (glass, steel, and carbon fibers), while the manufacturing process is relatively simple and does not require the addition of chemical additives [18]. Basalt fibers also exhibit high stiffness and elastic modulus, as well as good chemical and thermal stability, further supporting their potential as an alternative reinforcement for cementitious composites [15,16,19,20].

In this regard, basalt fiber-reinforced concrete (BFRC) is a relatively recent material that has demonstrated promising mechanical performance. Previous studies have reported improvements in compressive strength, tensile strength, flexural strength, toughness index, fracture energy, flexural-to-compressive strength ratio, and reinforcement coefficient of concrete incorporating basalt fibers at volume fractions of 0.3% and 0.4% [20,21]. Ja'e et al. [22] reported improvements in the mechanical properties of concrete containing basalt fibers and silica fume, with increases ranging from 28% to 65% in compressive strength and from 11% to 46% in flexural strength. Ögüt and Demir [23] investigated the influence of basalt fiber contents of 1–3% (wt.%) on the mechanical and durability properties of concrete and reported that the fibers improved flexural performance and corrosion resistance, while their effect on compressive strength was limited. However, other authors have indicated that fiber incorporation alone is not the most effective approach for enhancing the compressive strength of concrete [24].

The performance of the basalt fiber-reinforced concrete is linked to the fiber–matrix interaction, since adequate bonding is required for efficient stress transfer between the fibers and the cementitious matrix [25]. One possible approach to improve this interaction is the application of surface treatments to reduce surface imperfections and protect basalt fibers from the aggressive alkaline environment of the cementitious matrix [26]. These modifications can improve the interaction with the matrix by increasing surface roughness and specific surface area or by introducing functional chemical groups onto the fiber surface [27]. Manikandan et al. [28] reported that H_2SO_4 and NaOH treatments improved fiber–matrix adhesion, resulting in a 20% increase in tensile strength compared with composites containing untreated basalt fibers. However, aggressive chemical treatments may also reduce fiber integrity. Prolonged NaOH exposure has been reported to reduce basalt fiber strength by up to 80% [29]. Alternative surface modifications, such as aminosilane-based coatings,

have been shown to increase surface roughness and improve fiber–matrix adhesion [27]. More recently, Deng et al. [30] showed that HCl treatment increased basalt fiber surface roughness and improved dispersion within the cementitious matrix, with little effect on tensile properties.

Additionally, with the growing trend toward using more sustainable materials in cementitious composites, nanotechnology has attracted increasing attention in civil engineering for developing advanced materials and enhancing the properties and functionality of existing cement-based materials [31,32]. Nanomaterials can accelerate the cement hydration process, improving both the quality and quantity of hydration products, particularly calcium silicate hydrate (C–S–H) [33]. C–S–H is the predominant hydration product of Portland cement and is primarily responsible for the strength of cementitious materials. Since it constitutes approximately 50–60% of the solid volume of fully hydrated cement paste, any process that promotes additional C–S–H formation, such as the pozzolanic reaction of nanosilica, can enhance the mechanical performance of concrete [34].

To improve the mechanical properties of basalt fiber-reinforced concrete, researchers have proposed combining basalt fibers with nanosilica [35–37]. The synergistic use of these two materials can improve the fiber–matrix interfacial bond by refining the cementitious matrix, resulting in more efficient stress transfer and improved mechanical performance [38]. Colloidal nanosilica (NS), composed of nanoscale particles dispersed in a liquid medium, can provide improved dispersion compared with dry forms, promoting a more homogeneous distribution within the cementitious matrix [39]. In addition to enhancing the compressive strength of concrete, the incorporation of nanosilica can reduce its porosity by consuming calcium hydroxide (CH) through the pozzolanic reaction, leading to the formation of additional C–S–H [40,41]. Previous studies have also shown that the combined use of nanosilica and basalt fibers can improve the crack resistance of concrete by strengthening the fiber–matrix interfacial transition zone (ITZ) and enhancing stress transfer across cracks [33].

Nanosilica can also promote adhesion between the fibers and the cementitious matrix, thereby improving the reinforcement effect provided by the fibers [42]. Zhu et al. [43] determined an optimal combination of 6 mm basalt fibers at a content of 0.2% vol.% of concrete and 2% nanosilica by mass of cement. Their results indicated that NS effectively filled micropores in the concrete, increased matrix density, and improved the concrete's mechanical performance. Moreover, NS-induced micro- and nanostructures increased the surface roughness of basalt fibers, improving interaction with the cementitious matrix. However, the incorporation of nanosilica can reduce the workability of concrete [44].

In recycled concrete, the combined incorporation of nanosilica and basalt fibers has also been reported to enhance mechanical performance [45]. Flexural tests conducted on recycled concrete beams demonstrated that the simultaneous incorporation of nanosilica and basalt fibers improved structural performance by increasing load-carrying capacity while reducing crack width and deflection under loading [46]. In addition to material composition, temperature can affect the mechanical properties and microstructure of concrete. Deng et al. [47] and Lin et al. [48] reported changes in the mechanical behavior of recycled aggregate and conventional concrete, respectively, with a general reduction in compressive strength at elevated temperatures. Pehlivan [49] evaluated the combined incorporation of basalt fibers, nanosilica, and silica fume in cement mortars and found that basalt fibers improved flexural strength and toughness, while the combined use of nanosilica and silica fume enhanced the contribution of the fibers, resulting in a flexural strength increase of up to 23%. Sharaky et al. [50] investigated the influence of nanosilica content and mixing method on the strength and water absorption of concrete and reported that nanosilica increased compressive strength and reduced water absorption.

Based on the available literature, most studies have focused on the isolated effects of incorporating basalt fibers or nanosilica into cementitious composites. Hence, this study combines fiber length and content, surface treatment, and nanosilica incorporation within a sequential experimental approach. The present study aimed to evaluate the mechanical properties, microstructure, and capillary water absorption of basalt fiber-reinforced concrete. In the first stage, the effects of fiber length (3, 6, and 9 mm) and fiber content (0.1, 0.3, and 0.5% by mass of cement) on the compressive and flexural strengths of concrete were investigated to identify the best fiber configuration. Then, the basalt fibers from the configuration with the best mechanical performance were subjected to a surface treatment to improve their dispersion and interfacial bond with the cementitious matrix. In the third stage, the fiber configuration was combined with colloidal nanosilica (1.5 and 3.0% by mass of cement) to evaluate the combined influence of BF and NS on the compressive and flexural strengths of concrete, as well as on the fiber–matrix interfacial transition zone. In addition to the mechanical properties, the influence of the combined incorporation of basalt fibers and nanosilica on the capillary water absorption of concrete was also investigated.

2. Methodology

2.1. Materials

The Portland cement used in this study was the CPV-ARI by Votorantim (São Paulo, Brazil). This cement consists mainly of Portland clinker and calcium sulfate, with a maximum limestone filler content of 5%, according to ABNT NBR 16697:2018 [51]. Fine aggregate consisted of natural river sand from the Camaquã River, Rio Grande do Sul, Brazil, with a specific mass of 2.62 g/cm^3, fineness modulus of 1.81, and a maximum dimension of 2.36 mm. Coarse aggregate consisted of crushed rhyodacite rock from Caxias do Sul, Rio Grande do Sul, Brazil, with a specific mass of 2.47 g/cm^3, fineness modulus of 6.84, and a maximum dimension of 12.5 mm.

The basalt fiber (BF) used had three different lengths: 3, 6, and 9 mm. Table 1 presents their diameter and density. The density of the basalt fibers was experimentally determined by gas pycnometry using a Quantachrome Ultrapyc 1200e pycnometer (Company Anton Paar, Austrian company based in Graz, Austria) with nitrogen (N_2) as the analysis gas. The reported density values were calculated as the average of five measurement runs, with the corresponding standard deviations presented in Table 1. Basalt fiber diameters ranged from 12.01 to 20.01 µm, and their densities ranged from 1.958 to 2.470 g/cm^3. According to Xie et al. [33], basalt fibers used in concrete reinforcement present tensile strengths of 3000–4800 MPa and elastic moduli of 91–110 GPa.

Table 1. Basalt fiber properties.

BF	Diameter (µm)	Density (g/cm^3)
3 mm	12.01	1.958 ± 0.004
6 mm	20.01	2.470 ± 0.004
9 mm	12.67	2.256 ± 0.021

The samples were characterized by field-emission scanning electron microscopy (FEG-SEM) using a Tescan microscope (Brno, Czech Republic). The analyses were performed for each sample at the Central Laboratory of Microscopy (LCMIC) of the University of Caxias do Sul (UCS). Figure 1 shows the SEM images of (a) BF with a length of 3 mm, (b) BF with a length of 6 mm, (c) BF with a length of 9 mm, and (d) the characteristics of the three samples.

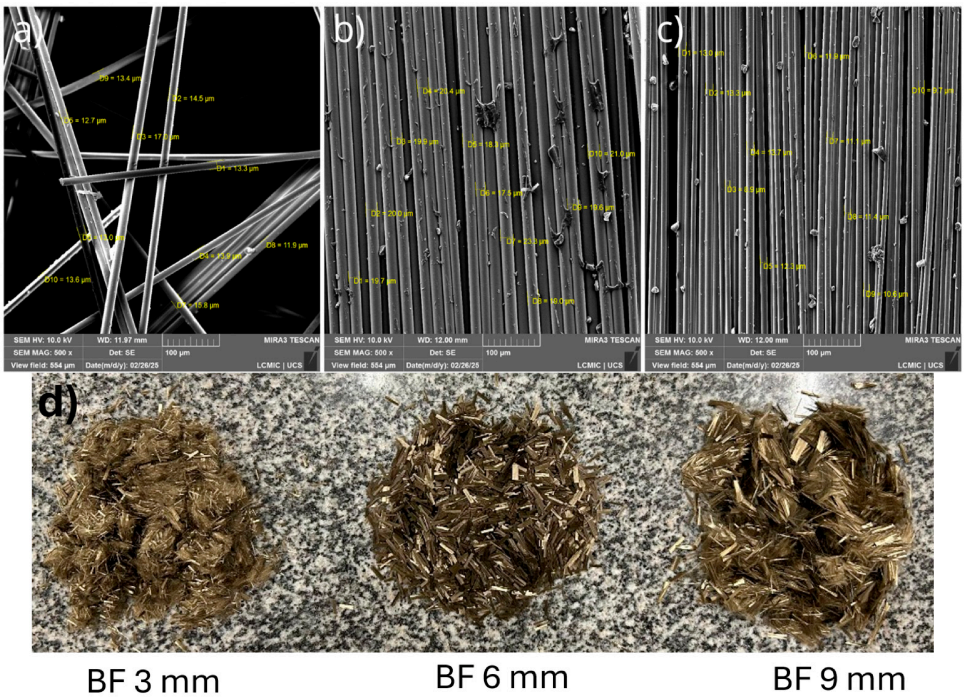


Figure 1. Basalt fibers with lengths of 3, 6, and 9 mm: (**a**) SEM image of 3 mm fibers; (**b**) SEM image of 6 mm fibers; (**c**) SEM image of 9 mm fibers; and (**d**) photographs of the three fiber samples.

The colloidal nanosilica (NS) used was SilicaFLOW Nano 40, provided by ADCO (São Paulo, Brazil). According to the manufacturer's specifications, the product contains approximately 40% solid SiO_2 and 60% water. The NS liquid was grey, with a density of 1.30–1.34 g/cm^3. The superplasticizer used was CALKOR, provided by Inkor (Santa Catarina, Brazil), containing 4–5% sodium resinate according to the manufacturer's specifications, with a dark color, a density of 1.03 g/cm^3, and a viscosity of 75–77 KU. The water-to-cement ratio and superplasticizer dosage were selected to ensure adequate workability for concrete casting, with the superplasticizer content proportionally increased as the basalt fiber content increased. The aggregate proportions were established considering previous studies [33] and the characteristics of the aggregates used in the present work.

2.2. Mixing

Basalt fiber-reinforced concrete (BFRC) was produced using three basalt fiber lengths (3, 6, and 9 mm). The BF contents were 0%, 0.1%, 0.3%, and 0.5% by mass of cement, with 0% corresponding to the reference concrete (RC). Considering the mixed proportions adopted for the reference concrete, the superplasticizer content was increased to maintain adequate concrete workability. The superplasticizer contents were 0.30%, 0.35%, and 0.40% for basalt fiber contents of 0.1%, 0.3%, and 0.5% (by mass of cement), respectively.

The abbreviation BFRC refers to basalt fiber-reinforced concrete. In the results section, the number immediately following BFRC indicates the fiber length (3, 6, or 9 mm), while the suffix after the hyphen indicates the basalt fiber content used in each mixture. Thus, mixtures containing fibers with lengths of 3, 6, and 9 mm were identified as BFRC3, BFRC6, and BFRC9, respectively, followed by the corresponding fiber content of 0.1%, 0.3%, or 0.5% by mass of cement.

After determining the most efficient basalt fiber configuration, the selected fiber length was used in the subsequent stage, in which the fibers were surface-treated. To improve the dispersion of basalt fibers in concrete, the basalt fiber surfaces were modified with a hydrochloric acid (HCl) solution. The basalt fibers were rinsed with deionized water to

remove any remaining grease from their surfaces. Then, the fibers were immersed in a 4 mol/L HCl solution at 50 °C for 10 h. After the treatment, the fibers were rinsed with deionized water and dried at 120 °C for 30 min. This treatment procedure was based on Deng et al. [30], who investigated different HCl concentrations, treatment temperatures, and immersion times. Using the same HCl concentration (4 mol/L) and temperature (50 °C) adopted in the present study, the authors reported an increase in basalt fiber surface roughness of approximately 163% after 15 h of treatment. They also demonstrated that HCl treatment improved fiber dispersion within the concrete matrix, with the dispersion coefficient increasing from 0.60 to 0.91. The nomenclature used for concrete reinforced with treated basalt fibers was BFRCT.

After evaluating the concrete reinforced with treated basalt fibers, colloidal nanosilica (NS) was incorporated as a partial replacement for cement at contents of 1.5% and 3.0% (by mass of cement). The superplasticizer content was slightly reduced in mixtures containing nanosilica compared with the corresponding mixtures containing only treated basalt fibers. For these mixtures, the NS content was included in the sample nomenclature. For example, BFRCT-0.3 + 1.5% NS indicates a concrete mixture containing 0.3% treated basalt fiber and 1.5% nanosilica, both expressed by mass of cement. The concrete mix proportions are shown in Table 2, while Figure 2 illustrates the mixing procedure adopted in this study, based on recommendations from [33]. The water content in Table 2 excludes the water from colloidal nanosilica (60% by mass). Considering both sources, the water-to-cement ratio remained around 0.57 for all mixtures.

Table 2. Concrete mix proportions for mixtures containing 3, 6, and 9 mm basalt fibers.

Concrete Specimens	Cement (kg/m^3)	Fine Aggregate (kg/m^3)	Coarse Aggregate (kg/m^3)	Water (kg/m^3)	SP (L/m^3)	BF (kg/m^3)	BFT (kg/m^3)	Colloidal NS (kg/m^3)
RC	425.0	900.0	920.0	242.0	1.07	0.0	0.0	0.0
BFRC-0.1	425.0	900.0	920.0	242.0	1.28	0.425	0.0	0.0
BFRC-0.3	425.0	900.0	920.0	242.0	1.50	1.275	0.0	0.0
BFRC-0.5	425.0	900.0	920.0	242.0	1.70	2.125	0.0	0.0
BFRCT-0.1	425.0	900.0	920.0	242.0	1.28	0.0	0.425	0.0
BFRCT-0.3	425.0	900.0	920.0	242.0	1.50	0.0	1.275	0.0
BFRCT-0.5	425.0	900.0	920.0	242.0	1.68	0.0	2.125	0.0
BFRCT-0.1 + 1.5% NS	418.6	900.0	920.0	230.0	1.26	0.0	0.42	16.00
BFRCT-0.3 + 1.5% NS	418.6	900.0	920.0	230.0	1.45	0.0	1.25	16.00
BFRCT-0.5 + 1.5% NS	418.6	900.0	920.0	230.0	1.66	0.0	2.10	16.00
BFRCT-0.1 + 3% NS	412.3	900.0	920.0	215.0	1.25	0.0	0.41	32.00
BFRCT-0.3 + 3% NS	412.3	900.0	920.0	215.0	1.45	0.0	1.24	32.00
BFRCT-0.5 + 3% NS	412.3	900.0	920.0	215.0	1.66	0.0	2.07	32.00

Note: BF and BFT contents of 0.1%, 0.3%, and 0.5% were calculated by mass of cement. NS contents of 1.5% and 3.0% were also calculated by mass of cement considering the solid content of the colloidal nanosilica (40%).

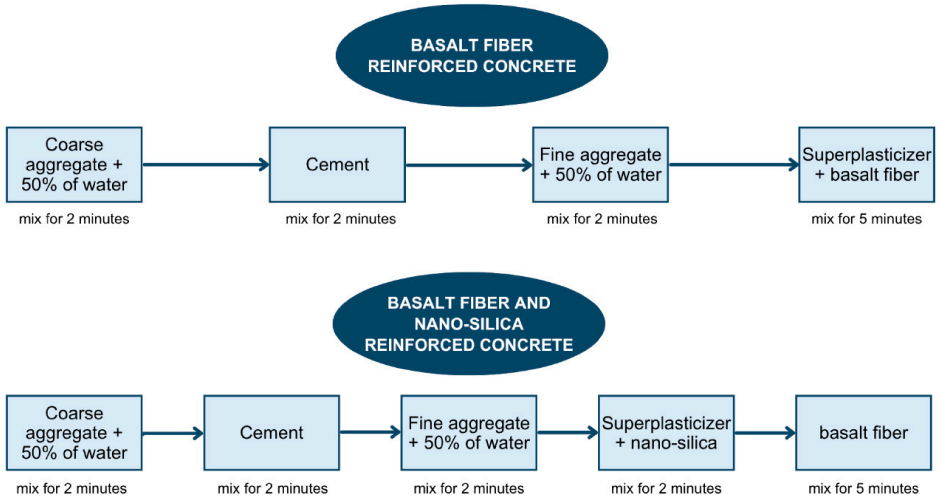


Figure 2. Mixing procedure for samples.

2.3. Preparation and Curing of Concrete Specimens

The concrete specimens were prepared according to the procedures described in the standards ABNT NBR 5738:2015 and 5739:2018 [52,53]. For the compressive strength tests, cylindrical specimens with dimensions of 100 mm in diameter and 200 mm in height were used. The molds were filled with two layers of concrete, with each layer compacted using 12 uniformly distributed strokes with a tamping rod. The specimens were stored on a flat surface for 24 h and then demolded. Subsequently, the specimens were stored in tanks containing a saturated aqueous solution of calcium hydroxide at a controlled temperature of 23 ± 2 °C until reaching 63 days of age.

For the flexural strength tests, the specimens were also prepared according to ABNT NBR 5738:2015 [52]. Prismatic specimens with dimensions of 100 mm in width, 100 mm in height, and 400 mm in length were used. The molds were filled with one layer of concrete and compacted using 75 strokes. The specimens were stored on a flat surface for 24 h and then demolded. Similar to the cylindrical specimens, they were stored in tanks containing a saturated aqueous solution of calcium hydroxide at a controlled temperature of 23 ± 2 °C until reaching 63 days of age. The curing age of 63 days was selected to evaluate the development of mechanical properties beyond the conventional 28-day period, allowing the investigation of the effects of basalt fibers and nanosilica over a longer curing period. The curing age of 63 days was also adopted in previous studies on fiber-reinforced cementitious composites [54].

In total, 228 cylindrical specimens (100 × 200 mm) and 76 prismatic specimens (100 × 100 × 400 mm) were produced in this study, including the reference concrete and all investigated concrete mixtures.

2.4. Workability Test

The slump test was performed to determine the consistency and workability of the concrete in the fresh state, according to the procedures established in the standard ABNT NBR 16889:2020 [55]. The concrete mixture was placed in a cone-shaped mold with a top diameter of 100 mm, a bottom diameter of 200 mm, and a height of 300 mm. The mold was filled in three layers of approximately equal height, with each layer compacted using 25 uniformly distributed strokes with a tamping rod. Immediately after removing the mold, the difference in height between the mold and the center of the concrete specimen was measured to determine the slump value.

2.5. Compressive and Flexural Strength

The compressive and flexural tensile strength tests were performed at LBTEC (UCS) using an EMIC PC 200 testing machine (São José dos Pinhais, Brazil). For the compressive strength test, cylindrical specimens with a diameter of 100 mm and a height of 200 mm were prepared following the procedures established in ABNT NBR 5739:2018 [53]. The compressive strength tests were performed at 7, 28, and 63 days to evaluate the evolution of compressive strength and the effects of different concrete mixtures. For each basalt fiber dosage, three specimens were tested at each age, resulting in a total of nine specimens per dosage.

For flexural tensile strength tests, prismatic specimens with dimensions of 100 mm in height, 100 mm in width, and 400 mm in length were prepared according to the procedures established in ABNT NBR 5738:2015 [52] for molding, compaction, and curing. The tests were performed according to ABNT NBR 12142:2010 [56], using a three-point bending configuration with a concentrated load applied at the center of a 300 mm support span. The tests were carried out on a servo-controlled press with hydraulic drive, model UH-501, Intermetric brand (Mogi das Cruzes, Brazil), with Tesc software. For each concrete mixture, two specimens were tested at 28 days and two at 63 days. The results were compared with those obtained for the reference concrete to evaluate the influence of the different basalt fiber contents and configurations on the flexural tensile strength.

2.6. Scanning Electron Microscopy (SEM)

SEM analysis was performed to evaluate the interaction between the fibers and the cementitious matrix using samples of basalt fiber-reinforced concrete, treated basalt fiber-reinforced concrete, and basalt fiber-reinforced concrete with nanosilica. FEG-SEM analyses were performed at the Central Microscopy Laboratory (LCMIC) of the University of Caxias do Sul (UCS) using a Tescan FEG Mira 3 scanning electron microscope (TESCAN Group, Brno, Czech Republic).

2.7. Water Absorption Test

The water absorption test was performed to evaluate the capillary water absorption behavior of the investigated concretes, following the procedures described in the standard ABNT NBR 9779:2012 [57]. Cylindrical specimens with dimensions of 100 mm in diameter and 200 mm in height were prepared according to NBR 5739:2018 [53]. After curing, the specimens were dried in an oven at 105 ± 5 °C until a constant mass was reached. Subsequently, the specimens were cooled to determine their dry mass. After determining the dry mass, the specimens were placed on supports in a container with a water level of approximately 5 mm, so that only one surface remained in contact with the water. During the test, the specimens were weighed after 72 h to determine the mass gain due to capillary water absorption. Water absorption was calculated as the ratio of the increase in mass to the surface area in contact with water, with the results expressed in g/cm^2. This procedure was used to evaluate water transport through the capillary pores and to analyze the influence of basalt fibers and nanosilica incorporation on the durability of the investigated concretes.

2.8. Statistical Analysis

A two-way analysis of variance (ANOVA) with replication was performed separately for each curing age and experimental stage, considering the investigated factors and their interactions. Three specimens per mixture were used for compressive strength and two specimens for flexural strength. A significance level of 5% ($p < 0.05$) was adopted. The effect size was calculated using partial eta-squared (η^2p), based on the sum of squares obtained from the ANOVA.

3. Results and Discussion

3.1. Workability

The workability of basalt fiber-reinforced concrete samples is an important parameter for ensuring adequate mixing and compaction while preventing material segregation. Figure 3 shows the effect of basalt fiber content by mass of cement and fiber length on concrete slump, and Figure 4 shows the effect of basalt fiber after treatment and the specimens with basalt fiber and nanosilica on concrete slump. The workability of fresh concrete is related to the amount of work required for its transport, placement, full compaction, and finishing. Generally, the addition of fibers reduces the workability of concrete [58]. The addition of fibers can decrease concrete workability, mainly due to the formation of a fiber network within the concrete mixture, which can restrict the movement of coarse aggregates and increase the resistance to mixture flow [58]. Katkhuda et al. [59] observed a reduction in slump with the addition of BF, which was attributed to the interlocking effect of the fibers and the absorption of part of the mixing water, resulting in increased friction between the fibers and the cementitious matrix.

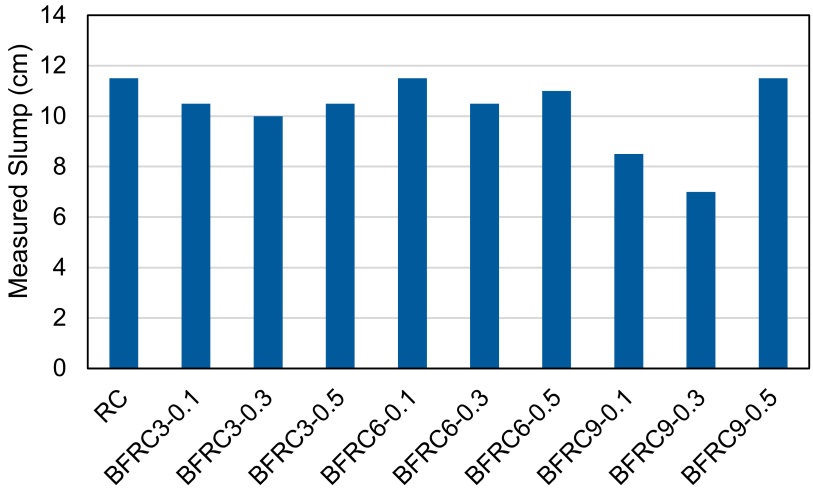


Figure 3. Effect of basalt fiber content and fiber length on concrete slump in relation to the reference concrete (RC).

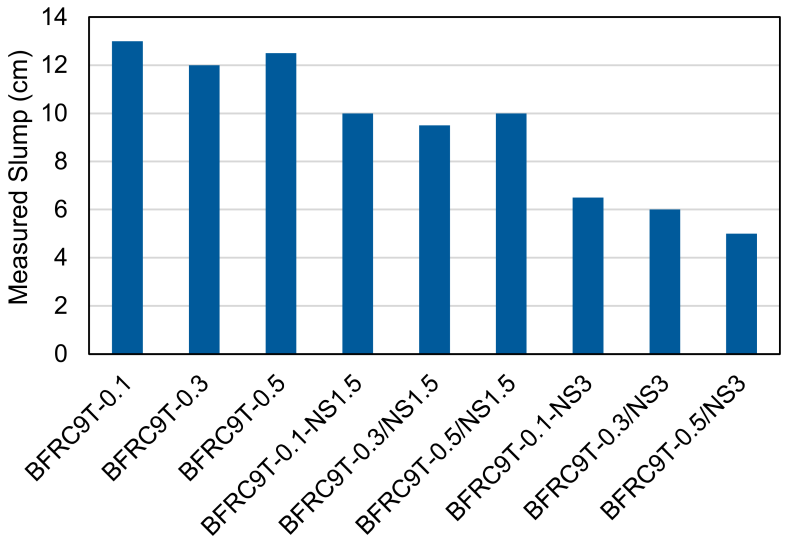


Figure 4. Effect of basalt fiber treatment and nanosilica addition on the slump of basalt fiber-reinforced concrete.

Figure 3 shows reduced workability in fiber-reinforced concrete mixtures with fiber contents of 0.1% and 0.3%. The mixtures containing 9 mm BF at contents of 0.1% and 0.3% showed reductions in workability of 26% and 39%, respectively. However, the specimens containing 0.5% basalt fiber showed slump values closer to those of the reference concrete, exhibiting unusual behavior with higher workability than the mixtures containing lower fiber contents. This behavior may be attributed to the slightly higher superplasticizer dosage used in mixtures containing 0.5% BF, which may have partially offset the reduction in workability caused by the higher fiber content. Since the superplasticizer dosage varied with fiber content, the influence of fiber content on workability cannot be evaluated independently of this variation. However, for the same fiber content, the superplasticizer dosage was kept constant across the different fiber lengths, allowing a direct comparison of the influence of fiber length on workability. Figure 4 shows that, after the basalt fiber treatment, workability increased by around 13%, 4.3%, and 8.7% for fiber contents of 0.1%, 0.3%, and 0.5% by mass o cement, respectively. For the mixtures containing nanosilica, a consistent reduction in workability was observed. For the mixture containing 0.5% basalt fiber and 3% NS, the slump decreased by 56.5%. For these mixtures, the superplasticizer dosage and other mix proportions were also adjusted with nanosilica incorporation, which should be considered when interpreting the workability results. This result was expected and is consistent with the behavior reported in previous studies [39].

3.2. Compressive Strength

3.2.1. Compressive Strength for Basalt Fiber-Reinforced Concrete

Figure 5 shows the compressive strength results for the reference concrete and the concrete samples reinforced with different basalt fiber lengths and fiber contents, expressed as percentages by mass of cement, at curing ages of 7, 28, and 63 days. All mixtures exhibited an increase in compressive strength with curing age, indicating that cement hydration progressed adequately throughout the curing period. However, none of the concretes reinforced with basalt fibers exceeded the compressive strength of the reference concrete. Mixtures containing 0.1% and 0.3% basalt fibers exhibited compressive strengths comparable to that of the reference concrete, with the BFRC9-0.1% mixture achieving 27.22 MPa at 63 days, which was almost identical to that of the reference concrete (27.21 MPa). On the other hand, concretes incorporating 0.5% basalt fibers exhibited a considerable reduction in compressive strength. Compared with reference concrete, reductions of 41.82%, 43.59%, and 41.60% were observed for the BFRC3-0.5%, BFRC6-0.5%, and BFRC9-0.5% mixtures, respectively, corresponding to an average decrease of about 42%. This reduction may be attributed to the higher fiber content, which can promote fiber agglomeration and the formation of local voids within the concrete matrix, thereby compromising its compressive strength. However, the higher superplasticizer dosage adopted for these mixtures may also have influenced the compressive strength results. Similar trends have been reported in the literature. Jyang et al. [58] observed reductions of 0.2% and 2.0% in compressive strength for concretes containing 0.1% and 0.3% basalt fibers (%vol.), respectively. Wang et al. [60] also reported a 23.2% reduction in compressive strength for concrete reinforced with 0.3% basalt fibers by mass of cement.

A two-way analysis of variance (ANOVA) was performed to evaluate the effects of basalt fiber length and content, as well as their interaction, on the compressive strength at 7, 28, and 63 days. Table 3 summarizes the results, including the degrees of freedom (df) and partial eta-squared values (η^2p). At all curing ages, both fiber length and fiber content had statistically significant effects on compressive strength ($p < 0.05$). Fiber content presented considerably higher F-values than fiber length at all curing ages, indicating that the variation associated with fiber content was more pronounced within the experimental

conditions investigated. This result is consistent with the considerable reduction in compressive strength observed in mixtures containing 0.5% BF. The partial eta-squared values also indicated a greater effect of fiber content ($\eta^2p = 0.969$) compared with fiber length ($\eta^2p = 0.576$) at 7 days. At 7 days, the interaction between fiber length and fiber content was also statistically significant ($p = 0.007$), indicating that the effect of one factor on early-age compressive strength depended on the level of the other factor. This interaction may be linked to differences in fiber dispersion and agglomeration associated with fiber length and content. Increasing the fiber content can promote the formation of fiber clusters and local voids, while different fiber lengths may influence their distribution within the cementitious matrix. At early curing ages, these local defects may have a greater influence on compressive strength since the cementitious matrix and the fiber–matrix interface are still developing. However, this interaction was not statistically significant at 28 ($p = 0.139$) and 63 days ($p = 0.308$), indicating no statistically significant interaction between fiber length and content at later curing ages.

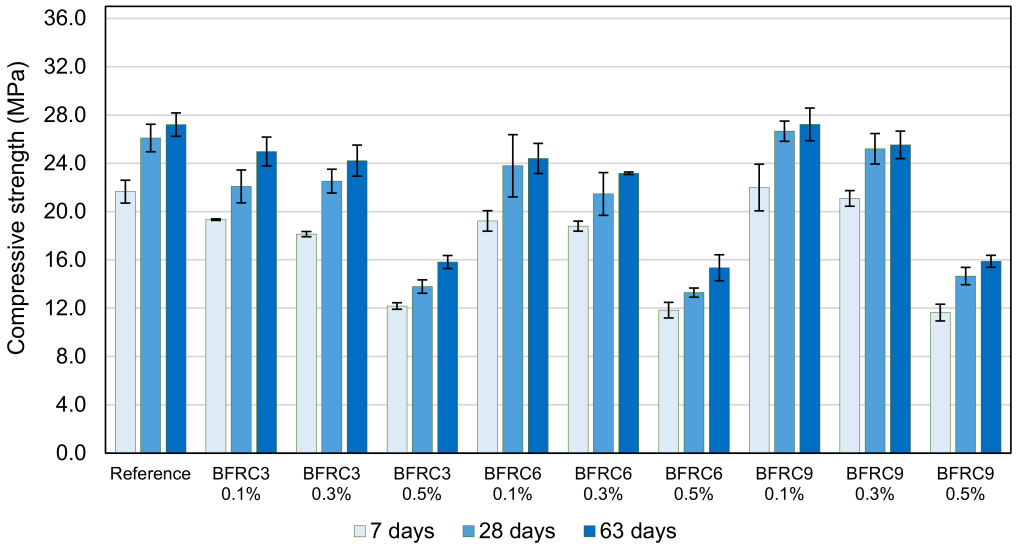


Figure 5. Compressive strength of basalt fiber-reinforced concrete with different fiber lengths and contents at 7, 28, and 63 days.

Table 3. ANOVA results for the compressive strength of basalt fiber-reinforced concrete at different curing ages.

Curing Age	Source of Variation	F-Value	*p*-Value	df	η^2p
7 days	Fiber length	12.238	<0.001	2, 18	0.576
	Fiber content	280.677	<0.001	2, 18	0.969
	Fiber length × fiber content	4.911	0.007	4, 18	0.522
28 days	Fiber length	12.223	<0.001	2, 18	0.576
	Fiber content	161.739	<0.001	2, 18	0.947
	Fiber length × fiber content	1.989	0.139	4, 18	0.306
63 days	Fiber length	7.956	0.003	2, 18	0.469
	Fiber content	245.839	<0.001	2, 18	0.965
	Fiber length × fiber content	1.299	0.308	4, 18	0.224

3.2.2. Compressive Strength for Treated Basalt Fiber-Reinforced Concrete (BFRCT)

Based on the BFRC results, the 9 mm basalt fiber was selected for subsequent stages, including fiber treatment followed by the incorporation of nanosilica, mainly due to its higher compressive strength compared with the other fiber lengths. Figure 6 shows the compressive strength results for concrete samples reinforced with 9 mm treated basalt fibers at curing ages of 7, 28, and 63 days. All mixtures exhibited an increase in compressive strength with curing age. However, the concrete samples reinforced with treated basalt fibers did not achieve the compressive strength of the reference concrete. The mixture containing 0.1% treated basalt fiber exhibited the lowest compressive strength, corresponding to a reduction of approximately 32.71% compared with the reference concrete at 63 days. In contrast, the mixtures incorporating 0.3% and 0.5% treated basalt fibers showed reductions of 17.49% and 18.93%, respectively, relative to the reference concrete.

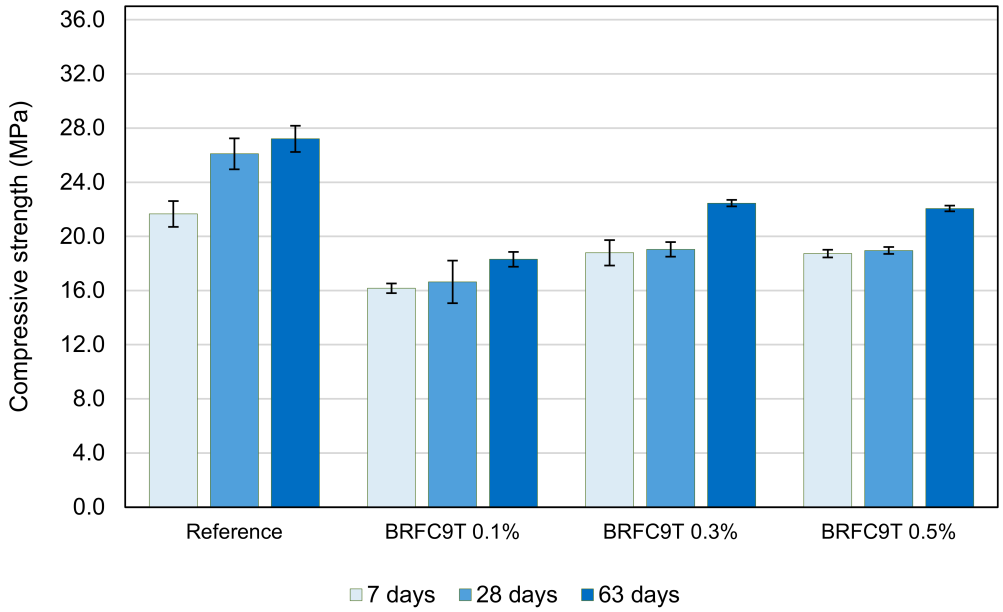


Figure 6. Compressive strength of 9 mm treated basalt fiber-reinforced concrete at 7, 28, and 63 days in relation to the reference concrete.

Increasing the fiber content from 0.3% to 0.5% caused only a small reduction in compressive strength, unlike the reduction observed when the untreated basalt fiber content increased from 0.1% to 0.5%. This behavior may indicate that the surface treatment contributed to improved fiber–matrix interaction and reduced adverse effects associated with fiber incorporation, such as fiber agglomeration. For mixtures containing 0.1% and 0.3% basalt fibers, fiber treatment did not yield higher compressive strength than the corresponding untreated mixtures. On the other hand, for the mixture containing 0.5% basalt fiber, the treatment increased the compressive strength by 38% compared with the corresponding untreated mixture at 63 days, indicating a positive effect of the surface treatment on the mechanical performance of the concrete at this fiber content.

A two-way analysis of variance (ANOVA) was also performed to evaluate the effects of fiber treatment and fiber content, as well as their interaction, on the compressive strength of concrete reinforced with 9 mm basalt fibers. The results are presented in Table 4. At 7 days, fiber treatment alone did not have a statistically significant effect ($p = 0.473$), whereas fiber content and the interaction between treatment and fiber content were statistically significant ($p < 0.001$). At 28 and 63 days, both factors and their interaction were statistically significant ($p < 0.001$), indicating that the effect of fiber treatment on compressive strength depended on the fiber content. The partial eta-squared values also indicated a strong interaction

between fiber treatment and fiber content at all curing ages (η^2p = 0.921–0.958). This behavior is consistent with the experimental results, in which the treatment did not improve the compressive strength of mixtures containing 0.1% and 0.3% BF, whereas an increase of approximately 38% was observed for the mixture containing 0.5% BF at 63 days compared with the corresponding untreated mixture. One possible explanation for this behavior is related to changes in fiber dispersion and fiber–matrix interactions after HCl treatment. At lower fiber contents, improved fiber dispersion may have a limited influence on compressive strength, whereas at higher contents, the greater tendency for fiber agglomeration may increase the potential benefits of surface treatment [30]. As cement hydration progresses, the development of the interfacial zone may further enhance this effect, contributing to the improvement observed for the mixture containing 0.5% treated BF at 63 days.

Table 4. Two-way ANOVA results for the compressive strength of untreated and treated 9 mm basalt fiber-reinforced concrete at different curing ages.

Curing Age	Source of Variation	F-Value	*p*-Value	df	η^2p
7 days	Fiber treatment	0.550	0.473	1, 12	0.044
	Fiber content	40.472	<0.001	2, 12	0.871
	Treatment × fiber content	70.263	<0.001	2, 12	0.921
28 days	Fiber treatment	74.988	<0.001	1, 12	0.862
	Fiber content	55.013	<0.001	2, 12	0.902
	Treatment × fiber content	87.412	<0.001	2, 12	0.936
63 days	Fiber treatment	26.875	<0.001	1, 12	0.691
	Fiber content	64.854	<0.001	2, 12	0.915
	Treatment × fiber content	137.048	<0.001	2, 12	0.958

3.2.3. Compressive Strength for Treated Basalt Fiber-Reinforced Concrete with Nanosilica (BFRCT-NS)

The results of the compressive strength tests for each basalt fiber-reinforced concrete mixture containing nanosilica at curing ages of 7, 28, and 63 days are presented in Figure 7. At earlier curing ages, the incorporation of nanosilica influenced the compressive strength. For mixtures containing 3.0% NS, the compressive strength ranged from 21.75 to 23.05 MPa at 7 days and increased to 25.57–27.39 MPa at 28 days, depending on the fiber content. Mixtures containing 1.5% NS showed a less consistent evolution over this period, particularly at 0.3% BF, for which the average compressive strength decreased from 22.28 to 20.55 MPa. These results indicate that the influence of nanosilica was already observed at earlier curing ages.

At 63 days, all mixtures containing 1.5% nanosilica by mass of cement exhibited lower compressive strength values than the reference concrete, whereas the mixtures containing 3.0% nanosilica exhibited higher compressive strength values than the reference concrete. The mixtures reinforced with treated 9 mm basalt fibers and incorporating 1.5% nanosilica exhibited compressive strengths that were 7.17%, 2.72%, and 11.03% lower than those of the reference concrete at 63 days for fiber contents of 0.1%, 0.3%, and 0.5%, respectively. On the other hand, the mixtures containing 3.0% nanosilica achieved compressive strengths that were 20.11%, 28.15%, and 19.70% higher than those of the reference concrete at the same fiber contents, respectively. Among the investigated mixtures, BFRCT9-0.3% + 3.0% NS exhibited the highest compressive strength at 63 days, an increase of 28.15% over the reference concrete. This behavior is consistent with the findings of Zheng et al. [61], who reported

that incorporating nanosilica improved the compressive strength of basalt fiber-reinforced concrete, even when mixtures containing only basalt fibers had lower compressive strength than the reference concrete. These results indicate a beneficial combined effect of treated basalt fibers and nanosilica on the compressive strength of the concrete, particularly at the 3.0% NS content. For all investigated fiber contents, increasing the nanosilica content from 1.5% to 3.0% resulted in higher compressive strength, suggesting that nanosilica contributed to compensating for the reduction in compressive strength associated with basalt fiber incorporation. This improvement may be associated with a denser cementitious matrix and an improved fiber–matrix interfacial transition zone (ITZ) promoted by nanosilica. Zheng et al. [61] also investigated the combined incorporation of BF and NS and reported that nanosilica can react with calcium hydroxide (CH) via the pozzolanic reaction, promoting the formation of additional calcium silicate hydrate (C–S–H), thereby contributing to a denser cementitious matrix and improved mechanical performance. Similarly, Wang et al. [36] reported that the combined incorporation of BF and NS improved the compressive strength of recycled concrete.

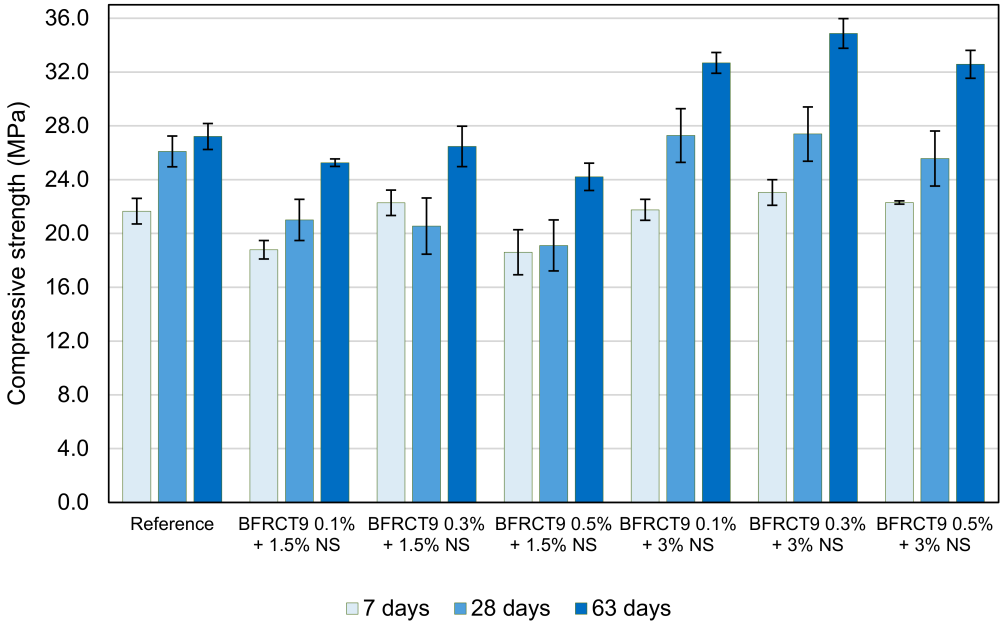


Figure 7. Compressive strength of 9 mm treated basalt fiber-reinforced concrete with different nanosilica and fiber contents at 7, 28, and 63 days.

A two-way analysis of variance (ANOVA) was performed to evaluate the effects of nanosilica and basalt fiber contents, as well as their interaction, on compressive strength. The results are presented in Table 5. Nanosilica content had a statistically significant effect at all curing ages ($p < 0.001$), with a considerably higher F-value at 63 days ($F = 482.991$). At 7 and 63 days, fiber content and the interaction between nanosilica and fiber content were also statistically significant ($p < 0.05$). In contrast, at 28 days, neither fiber content ($p = 0.386$) nor the interaction between the factors ($p = 0.227$) was statistically significant. The pronounced effect of nanosilica at 63 days is consistent with the higher compressive strength observed for the mixtures containing 3.0% NS. This behavior may be associated with the filler effect and the pozzolanic activity of nanosilica, which can promote matrix densification and the formation of additional C–S–H as curing progresses.

Table 5. Two-way ANOVA results for the compressive strength of basalt fiber-reinforced concrete containing nanosilica at different curing ages.

Curing Age	Source of Variation	F-Value	*p*-Value	df	η^2p
7 days	Nanosilica content	59.852	<0.001	2, 18	0.869
	Fiber content	18.457	<0.001	2, 18	0.672
	NS × fiber content	4.617	0.010	4, 18	0.506
28 days	Nanosilica content	63.581	<0.001	2, 18	0.876
	Fiber content	1.005	0.386	2, 18	0.100
	NS × fiber content	1.563	0.227	4, 18	0.258
63 days	Nanosilica content	482.991	<0.001	2, 18	0.982
	Fiber content	19.784	<0.001	2, 18	0.687
	NS × fiber content	6.652	0.002	4, 18	0.596

3.3. Flexural Strength

3.3.1. Flexural Strength for Basalt Fiber Reinforced Concrete

The results of the flexural tensile strength tests for each basalt fiber-reinforced concrete mixture containing 3, 6, and 9 mm fibers at contents of 0.1%, 0.3%, and 0.5% by mass of cement, at curing ages of 28 and 63 days, are presented in Figure 8. In flexural loading, basalt fibers can act as bridges across cracks, contributing to stress transfer after crack initiation. Among the mixtures containing 3 mm fibers (BFRC3), the addition of 0.1% BF resulted in a slight increase in flexural strength compared with the reference concrete, reaching 7.17 MPa at 63 days. Increasing the fiber content to 0.3% for the 3 mm BF reduced the flexural strength, whereas the mixture containing 0.5% BF reached 7.29 MPa at 63 days, corresponding to an increase of about 4.3% compared with the reference concrete.

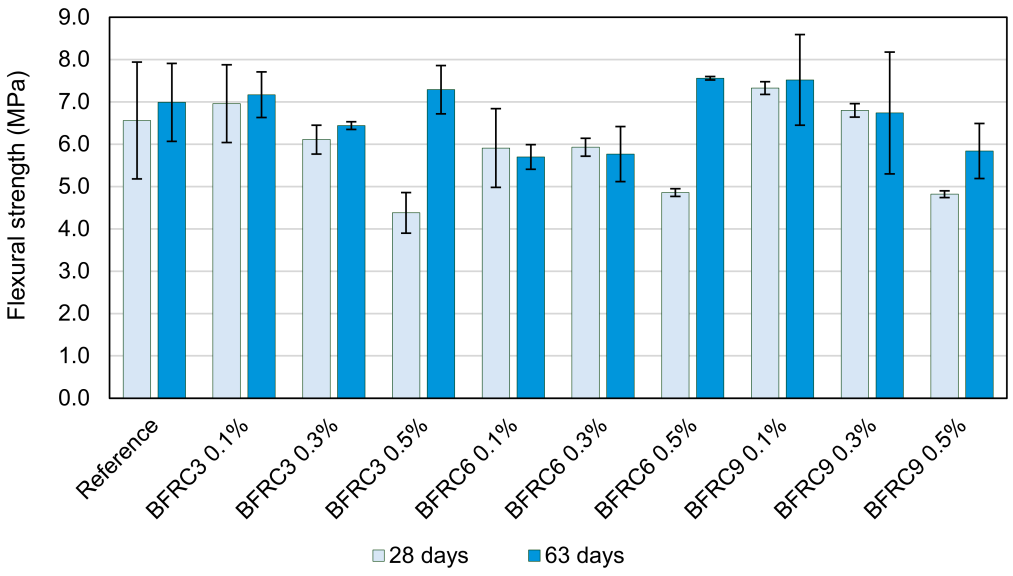


Figure 8. Flexural strength of basalt fiber-reinforced concrete with different fiber lengths and contents at 28 and 63 days.

For the mixtures containing 6 mm fibers (BFRC6), the specimens with 0.1% and 0.3% BF exhibited lower flexural strengths than the reference concrete at 63 days, with reductions of about 18.5% and 17.5%, respectively. On the other hand, the mixture containing 0.5% BF showed a considerable increase in flexural strength between 28 and 63 days, reaching 7.56 MPa at 63 days, around 8.3% higher than the reference concrete. A similar increase between curing ages was observed for all mixtures containing 0.5% BF, with increases

of around 66.4%, 55.5%, and 21.2% for BFRC3, BFRC6, and BFRC9, respectively. For the mixtures containing 9 mm fibers (BFRC9), the best performance was achieved with 0.1% BF, reaching 7.52 MPa at 63 days, representing a 7.6% increase over the reference concrete. Increasing the fiber content to 0.3% and 0.5% with 9 mm BF resulted in lower flexural strength values. In particular, BFRC9-0.5% exhibited a 16.5% reduction compared with the reference concrete at 63 days. This may be associated with difficulties in fiber dispersion at higher fiber contents, which can reduce the efficiency of stress transfer within the cementitious matrix [45]. Similar trends have been reported in the literature. Niu et al. [62] observed reductions of up to 11% in flexural strength with the incorporation of 0.2% BF (%vol.), while Jiang et al. [58] reported improvements in flexural strength up to a BF content of 0.3% (%vol.) and better performance with longer fibers. Algin and Ozen [17] also reported an increase of up to 15.3% using 0.3% (%vol.) of 6 mm basalt fibers.

A two-way analysis of variance (ANOVA) was performed to evaluate the effects of basalt fiber length and content, as well as their interaction, on flexural strength. The results are presented in Table 6. At 28 days, both fiber length ($p = 0.040$) and fiber content ($p < 0.001$) had statistically significant effects on flexural strength, whereas their interaction was not statistically significant ($p = 0.165$). Fiber content presented a higher F-value than fiber length, indicating a more pronounced variation associated with this factor. The influence of fiber length may be related to differences in fiber anchorage and fiber–matrix interaction, while the effect of fiber content may be associated with the amount of fibers available for crack bridging, as well as changes in workability and fiber dispersion at higher contents. It is important to note that the statistical significance of fiber content does not imply a continuous increase in flexural strength with increasing BF content, but rather that changes in fiber content affect the mechanical response. At 63 days, neither fiber length ($p = 0.376$) nor fiber content ($p = 0.380$) had a statistically significant effect on flexural strength. Their interaction was also not statistically significant ($p = 0.064$). Therefore, although differences in flexural strength were observed among the individual mixtures at 63 days, these differences were insufficient to demonstrate statistically significant main effects of fiber length or content under the conditions investigated. The ANOVA results for flexural strength should be interpreted with caution due to the limited number of specimens tested per mixture (n = 2).

Table 6. Two-way ANOVA results for the flexural strength of basalt fiber-reinforced concrete at different curing ages.

Curing Age	Source of Variation	F-Value	*p*-Value	df	η^2p
28 days	Fiber length	4.716	0.040	2, 9	0.512
	Fiber content	37.660	<0.001	2, 9	0.893
	Fiber length × fiber content	2.086	0.165	4, 9	0.481
63 days	Fiber length	1.092	0.376	2, 9	0.195
	Fiber content	1.080	0.380	2, 9	0.194
	Fiber length × fiber content	3.275	0.064	4, 9	0.593

3.3.2. Flexural Strength for Treated Basalt Fiber Reinforced Concrete

Figure 9 presents the flexural strength results for concrete samples reinforced with treated 9 mm basalt fibers at curing ages of 28 and 63 days. All mixtures exhibited an increase in flexural strength with curing age. However, all concretes reinforced with treated basalt fibers showed lower flexural strength than the reference concrete. Among the treated fiber mixtures, the best performance was obtained with BFRCT9-0.5%, which reached

5.36 MPa at 63 days. Nevertheless, this value was around 23.32% lower than that of the reference concrete. Despite the increase in flexural strength with curing age, all mixtures containing treated 9 mm basalt fibers exhibited lower values at 63 days than the corresponding mixtures containing untreated 9 mm fibers. It is interesting to note that the untreated BFRC9 mixtures showed a reduction in flexural strength with increasing fiber content, whereas the treated BFRCT9 mixtures showed an increase from 4.86 MPa at 0.1% BF to 5.36 MPa at 0.5% BF. This change in behavior suggests that the surface treatment modified the effect of fiber content on the flexural response, possibly due to changes in fiber dispersion and fiber–matrix interactions. However, under the conditions investigated, the treatment did not improve the overall flexural strength relative to the untreated fibers. This reduction may be associated with changes in the interfacial bond after HCl treatment, since improved fiber dispersion does not necessarily result in more efficient stress transfer between the fibers and the cementitious matrix. As discussed by Iorio et al. [27] and Manikandan et al. [28], the characteristics of the fiber–matrix interface influence the mechanical performance of composites, particularly through mechanisms such as interfacial debonding and fiber pull-out. These mechanisms may have contributed to the lower flexural strength observed for the treated fiber mixtures.

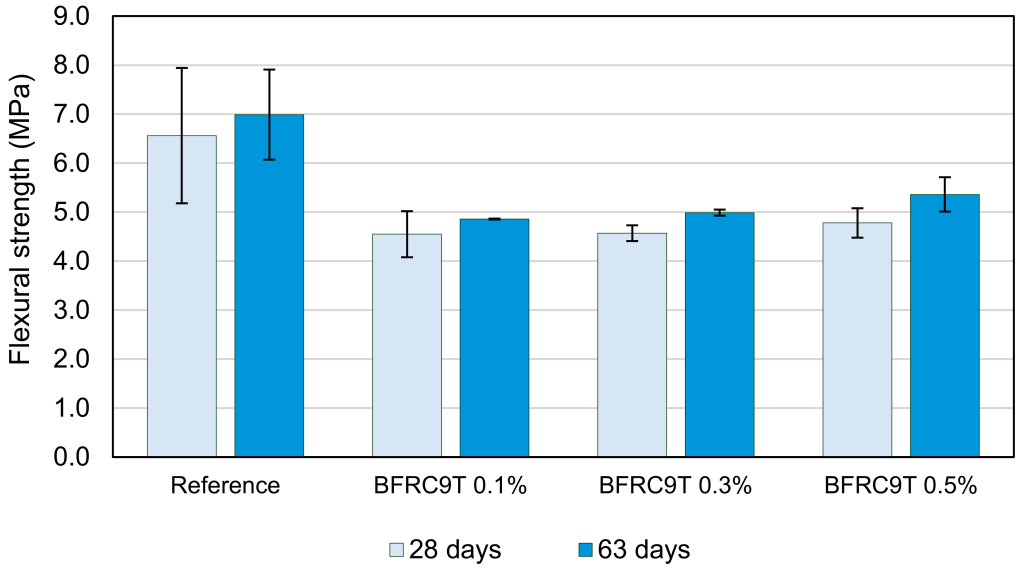


Figure 9. Flexural strength of concrete reinforced with treated 9 mm basalt fibers at different fiber contents at 28 and 63 days.

A two-way ANOVA was performed to evaluate the effects of fiber treatment and fiber content on flexural strength (Table 7). At 28 days, fiber treatment, fiber content, and their interaction had statistically significant effects ($p < 0.05$), with fiber treatment presenting the highest F-value. The significant interaction indicates that the treatment effect depended on the fiber content at this curing age, which may be associated with changes in fiber–matrix interactions promoted by the surface treatment. At 63 days, only fiber treatment remained statistically significant ($p = 0.012$), whereas fiber content ($p = 0.600$) and the interaction between treatment and fiber content ($p = 0.231$) were not significant. Although the surface treatment affected the flexural response, it did not improve flexural strength, as the treated fiber mixtures exhibited lower values than the corresponding untreated mixtures.

Table 7. Two-way ANOVA results for the flexural strength of untreated and treated 9 mm basalt fiber-reinforced concrete at different curing ages.

Curing Age	Source of Variation	F-Value	*p*-Value	df	η^2p
28 days	Fiber treatment	130.106	<0.001	1, 6	0.956
	Fiber content	22.030	0.002	2, 6	0.880
	Treatment × fiber content	32.136	<0.001	2, 6	0.915
63 days	Fiber treatment	12.694	0.012	1, 6	0.679
	Fiber content	0.556	0.600	2, 6	0.156
	Treatment × fiber content	1.892	0.231	2, 6	0.387

3.3.3. Flexural Strength for Basalt Fiber-Reinforced Concrete with Nanosilica

The flexural strength results for concrete samples reinforced with treated 9 mm basalt fibers at contents of 0.1%, 0.3%, and 0.5%, and incorporating 1.5% and 3.0% nanosilica, all by mass of cement, at curing ages of 28 and 63 days are presented in Figure 10. At 28 days, the mixtures containing 3.0% NS exhibited average flexural strengths of 6.22, 6.23, and 5.83 MPa for fiber contents of 0.1%, 0.3%, and 0.5%, respectively. These values were higher than those obtained with 1.5% NS (5.86, 5.18, and 5.03 MPa), showing that nanosilica content already influenced flexural strength at 28 days. At 63 days, all mixtures containing 1.5% NS exhibited lower flexural strength than the reference concrete. The mixtures containing 0.1%, 0.3%, and 0.5% treated BF exhibited reductions of about 17.7%, 14.2%, and 20.6%, respectively, relative to the reference concrete. However, better performance was observed with the incorporation of 3.0% NS. The mixtures containing 0.1% and 0.5% treated BF and 3.0% NS presented flexural strengths around 8.2% and 5.2% lower values than the reference concrete, respectively, whereas BFRCT9-0.3% + 3.0% NS reached 7.57 MPa at 63 days, representing an increase of 8.3% compared with the reference concrete. This mixture presented the highest flexural strength among all mixtures investigated in this study.

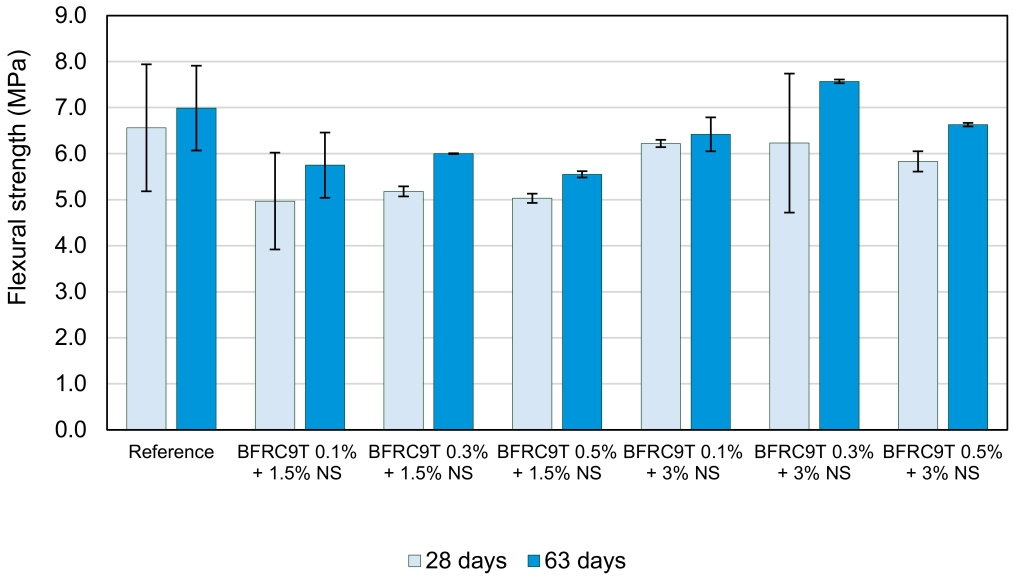


Figure 10. Flexural strength of treated basalt fiber-reinforced concrete containing nanosilica at 28 and 63 days.

The improved performance observed with 3.0% NS may be attributed to the combined effects of fiber–matrix interaction and microstructural refinement induced by nanosilica. Nanosilica can contribute to a denser cementitious matrix through its filler and pozzolanic effects, while the surface treatment may influence fiber dispersion and fiber–matrix interaction. These mechanisms are further discussed in light of the SEM microstructural analysis. Similar behavior was reported by Chen [45] who observed a 9.26% increase in flexural strength in recycled aggregate concrete containing 0.3% BF and 3.0% NS (%vol.). Abna and Mazloom [63] also reported a 22% improvement in flexural strength with the combined incorporation of polypropylene fibers and nanosilica.

A two-way ANOVA was performed to evaluate the effects of nanosilica and basalt fiber contents on flexural strength (Table 8). At 28 days, only nanosilica content had a statistically significant effect ($p = 0.018$), whereas fiber content and the interaction between the factors were not significant ($p > 0.05$). This result indicates that the differences in flexural strength at this curing age were primarily associated with the nanosilica content, possibly due to its contribution to microstructural refinement of the cementitious matrix and the fiber–matrix interfacial zone. At 63 days, both nanosilica ($p < 0.001$) and fiber contents ($p = 0.039$) had statistically significant effects, with nanosilica presenting a higher F-value. The more pronounced influence of nanosilica at this age may be associated with the progression of hydration and pozzolanic reactions, contributing to a denser cementitious matrix. In this condition, the amount of fibers available for crack bridging may also become relevant to the flexural response. The interaction between nanosilica and fiber content was not statistically significant at either 28 or 63 days ($p > 0.05$).

Table 8. Two-way ANOVA results for the flexural strength of treated basalt fiber-reinforced concrete containing nanosilica at different curing ages.

Curing Age	Source of Variation	F-Value	*p*-Value	df	η^2p
28 days	Nanosilica content	6.521	0.018	2, 9	0.592
	Fiber content	0.344	0.718	2, 9	0.071
	NS × fiber content	0.363	0.829	4, 9	0.139
63 days	Nanosilica content	58.145	<0.001	2, 9	0.928
	Fiber content	4.732	0.039	2, 9	0.513
	NS × fiber content	3.382	0.060	4, 9	0.601

3.4. Water Absorption by Capillarity

The water absorption by capillarity test was performed at 72 h to evaluate capillary water absorption in the different concrete mixtures. The results obtained are presented in Figure 11. The reference concrete exhibited a capillary water absorption of 0.81 g/cm^2 after 72 h. From the results, it is evident that basalt fiber-reinforced concrete showed no linear relationship between fiber content and capillary water absorption. For the 3- and 6-mm fibers, the mixtures containing 0.5% BF exhibited relatively low absorption values of around 0.4 g/cm^2 after 72 h. However, the 9 mm fiber mixtures showed a different behavior, indicating that capillary water absorption was not governed solely by fiber content. These results indicate that the reduction in compressive strength observed at higher fiber contents was not necessarily accompanied by increased capillary water absorption. This behavior may be related to differences between local defects affecting mechanical strength and the pore connectivity governing capillary water transport.

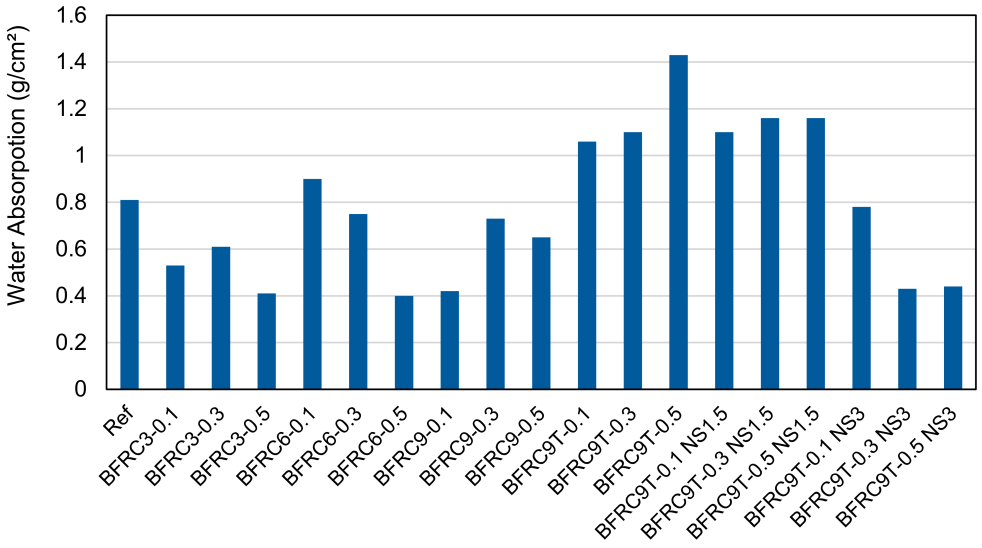


Figure 11. Water absorption by capillarity of the concrete mixtures after 72 h.

The mixtures containing treated 9 mm basalt fibers showed a higher water absorption than the corresponding untreated fiber mixtures, reaching up to 1.40 g/cm^2. Although the surface treatment modified the fiber–matrix interaction, it did not reduce capillary water absorption under the investigated conditions. This may be associated with changes in the surface characteristics of basalt fibers after HCl treatment. Deng et al. [30] reported that HCl treatment increased the surface wettability of basalt fibers, as indicated by the reduction in contact angle. Ravel et al. [64] also demonstrated that changes in the surface properties of basalt fibers after thermal treatment increased capillary pressure, indicating the influence of surface modification on water transport. This higher wettability may favor water interaction with the fiber surfaces and contribute to capillary water absorption. In addition, water absorption depends on the porosity and connectivity of pores within the cementitious matrix.

The incorporation of nanosilica changed the water absorption behavior. With 1.5% NS, similar absorption values were achieved among the different fiber contents. For cases with 3.0% NS, capillary water absorption decreased with higher fiber content, from 0.78 g/cm^2 at 0.1% BF to 0.40–0.45 g/cm^2 at 0.3–0.5% BF. This may be attributed to changes in the fiber–matrix interaction and pore structure. However, the individual contribution of fiber content to this reduction cannot be isolated from the other mixture variables. The lower water absorption observed with 3.0% NS may be associated with the filler and pozzolanic effects of nanosilica, which contribute to a denser cementitious matrix and may promote pore structure refinement. This is also consistent with the improved mechanical performance observed for the mixtures containing 3.0% NS.

3.5. Microstructure

The microstructure of the basalt fiber-reinforced concrete mixtures was evaluated using SEM to investigate fiber distribution, fiber–matrix interactions, and the characteristics of the cementitious matrix. Figure 12 shows SEM images of the concrete reinforced with untreated basalt fibers. From Figure 12a, it is possible to observe fiber agglomeration and voids between the fibers, indicating non-uniform fiber dispersion within the cementitious matrix. Fiber agglomeration can contribute to the formation of voids and reduce workability, consequently affecting the mechanical properties of fiber-reinforced concrete, as also reported by Qin and Wu [65]. These observations are consistent with the reduction in mechanical performance observed by some BFRC mixtures at higher fiber contents. Figure 12b presents

the SEM image of concrete reinforced with 0.3% of 3 mm basalt fibers. The microstructure shows the presence of pores and voids within the cementitious matrix, which may provide pathways for water transport and contribute to the capillary water absorption behavior observed experimentally.

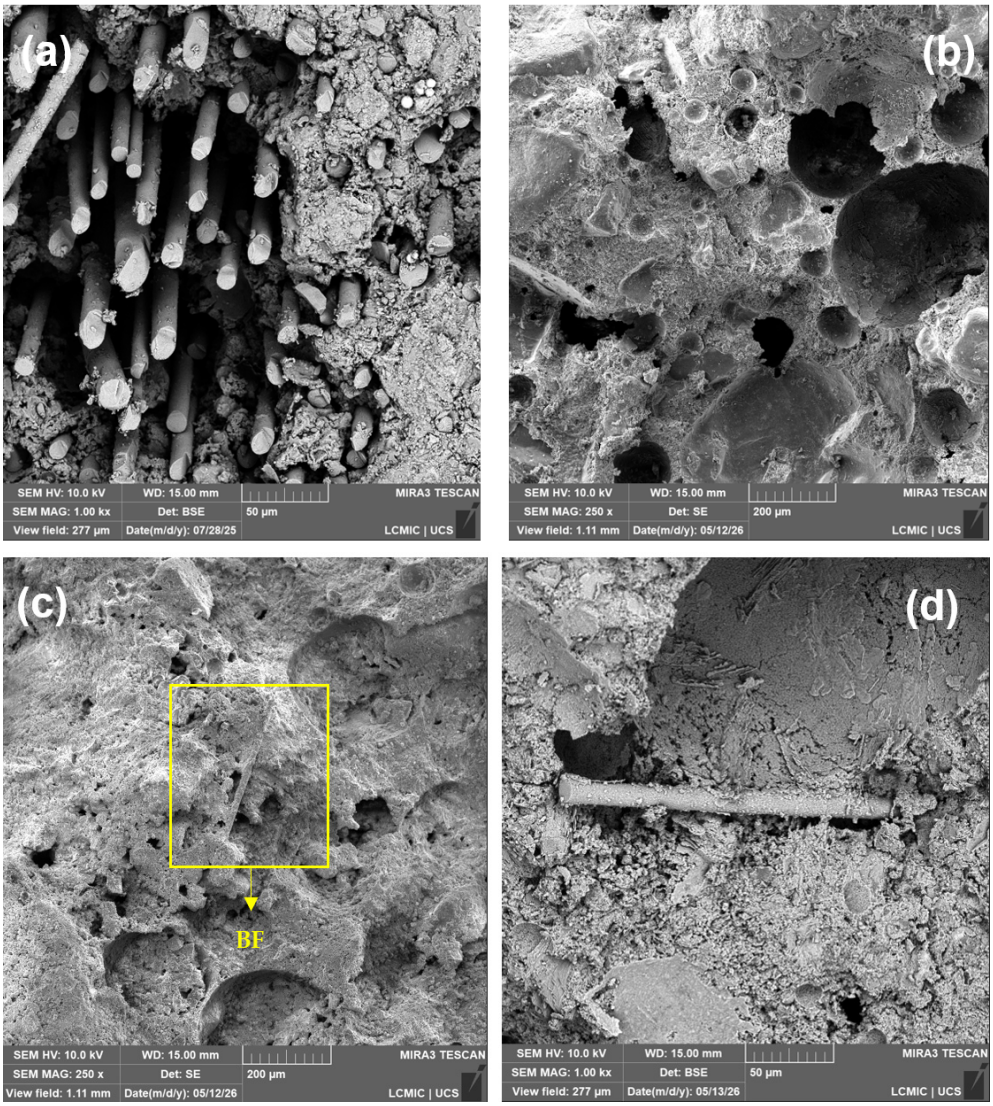


Figure 12. SEM image of basalt fiber-reinforced concrete: (**a**) BFRC 3 mm at 1000×; (**b**) BFRC 3 mm and 0.3% at 250×; (**c**) BFRC 3 mm and 0.5% SEM at 250×; (**d**) BFRC 9 mm and 0.1% SEM at 1000×.

Despite the presence of fiber agglomeration and voids, SEM images also show regions where the cementitious matrix surrounds the basalt fibers (Figure 12c,d). The cement paste can be observed surrounding the fibers, with cementitious products deposited on their surfaces. These products may increase interfacial friction and contribute to the fiber–matrix bond. According to Shi et al. [66], improved interfacial interaction between basalt fibers and the cementitious matrix can contribute to stress transfer and restrict crack propagation. However, interfacial voids are still visible in some regions around the untreated fibers, indicating locally incomplete contact between the fibers and the matrix. These microstructural characteristics may help explain the variability in the mechanical and capillary water absorption results observed for the untreated BFRC mixtures.

The microstructure changed with the incorporation of treated 9 mm basalt fibers and 3.0% nanosilica, as shown in Figure 13. The SEM images suggest a more compact cementitious matrix in the examined regions surrounding the treated basalt fibers, with

some visible interfacial voids, compared with the untreated BFRC mixtures shown in Figure 12. However, these observations are qualitative, and the different imaging conditions do not allow a direct quantitative comparison of matrix density or porosity. At higher magnifications (Figure 13b,d), deposits can be observed around the fiber surfaces. The denser microstructure observed with nanosilica is consistent with previous studies reporting that nanosilica can reduce porosity and refine the cementitious matrix through its filler and pozzolanic effects [36]. Still, these mechanisms were not directly confirmed in the present study. These microstructural results provide qualitative information that complements the mechanical and capillary water absorption results obtained in this study. The mixture containing 0.3% treated 9 mm BF and 3.0% NS presented the highest compressive and flexural strengths, while the mixtures containing 3.0% NS also exhibited lower capillary water absorption, particularly at fiber contents of 0.3% and 0.5%. In this regard, the improved mechanical performance and reduced capillary water absorption observed with 3.0% NS may be associated with a more compact cementitious matrix and better fiber–matrix contact in the examined regions, as suggested by the qualitative SEM observations.

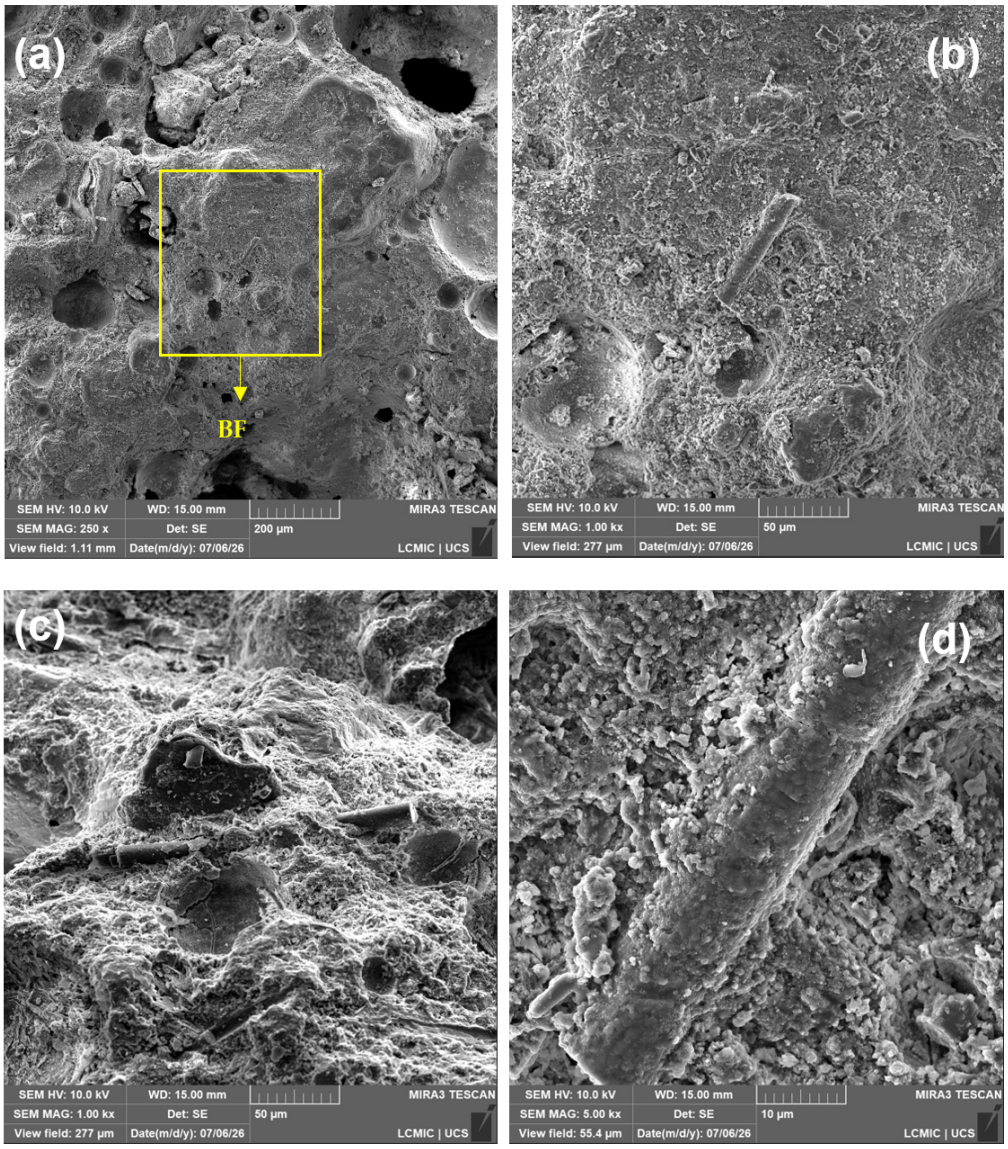


Figure 13. SEM images of treated basalt fiber-reinforced concrete containing 3.0% nanosilica: (**a**) BFRCT9-0.1 at 250×; (**b**) BFRCT9-0.1 at 1000×; (**c**) BFRCT9-0.5 at 1000×; and (**d**) BFRCT9-0.5 at 5000×.

4. Conclusions

This study investigated the combined effects of basalt fiber length, fiber content, surface treatment, and the addition of nanosilica on the workability, mechanical properties, capillary water absorption, and concrete microstructure. Basalt fibers with lengths of 3, 6, and 9 mm were initially evaluated at contents of 0.1%, 0.3%, and 0.5% by mass of cement. Based on the mechanical performance, 9 mm fibers were selected for surface treatment, followed by the incorporation of 1.5% and 3.0% nanosilica by mass of cement. The concrete mixtures were evaluated through slump, compressive and flexural strength tests, capillary water absorption, and SEM analysis. Based on the experimental results, the main conclusions are summarized as follows:

1. The incorporation of basalt fibers affected the workability and mechanical properties of concrete. Fiber length and fiber content impacted compressive strength, while higher fiber contents reduced workability. Among the untreated BFRC mixtures, low and intermediate fiber contents yielded better mechanical performance, whereas incorporating 0.5% BF reduced compressive strength. SEM observations suggested the presence of fiber agglomeration and voids in some regions, which may contribute to this behavior.
2. The surface treatment of the basalt fibers modified the effect of fiber content on the mechanical properties of concrete. At 63 days, the treatment increased compressive strength by 38% for the mixture containing 0.5% BF compared with the corresponding untreated mixture. However, no improvement was observed at lower fiber contents, and all treated fiber mixtures exhibited lower flexural strength than their untreated counterparts. The treated BF mixtures also exhibited higher capillary water absorption than the untreated samples.
3. The incorporation of nanosilica improved the mechanical properties and capillary water absorption of concrete containing treated basalt fibers. Mixtures containing 1.5% nanosilica did not outperform the reference concrete in mechanical performance, whereas those incorporating 3.0% nanosilica exhibited higher compressive strength for all investigated fiber contents and improved flexural performance, particularly at 0.3% BF. The mixtures containing 3.0% NS also presented lower capillary water absorption, especially at fiber contents of 0.3% and 0.5%.
4. The combination of 0.3% treated 9 mm basalt fibers with 3.0% nanosilica provided the highest compressive and flexural strengths among the investigated mixtures. At 63 days, the compressive strength increased from 27.21 to 34.87 MPa, representing a 28.2% increase over the reference concrete. The flexural strength reached 7.57 MPa, representing an 8.3% increase over the reference value of 6.99 MPa.
5. SEM images suggested that the mixtures containing treated basalt fibers and 3.0% nanosilica exhibited a denser and more compact cementitious matrix, with fewer visible interfacial voids and good contact between the fibers and the surrounding matrix compared with the untreated BFRC mixtures. These microstructural characteristics are consistent with the improved mechanical performance and lower capillary water absorption observed for the mixtures containing 3.0% nanosilica.

Finally, the results presented in this work demonstrated that the performance of basalt fiber-reinforced concrete depends not only on fiber length and content but also on the characteristics of the cementitious matrix. The combined use of treated 9 mm basalt fibers and 3.0% nanosilica showed favorable results in terms of mechanical strength, microstructural observations, and capillary water absorption under the experimental conditions investigated.

To continue this work, future studies could compare colloidal and dry nanosilica to investigate the influence of their physical form on the mechanical and durability properties of

basalt fiber-reinforced concrete. Further investigations could also evaluate the effects of HCl treatment on fiber surface properties, mechanical integrity, long-term alkaline resistance, and residual chloride content, as well as the environmental impacts associated with acid consumption and waste generation. In addition, future studies could compare the CO_2 emissions and energy consumption associated with the production of basalt, steel, and glass fibers to evaluate their environmental performance as concrete reinforcement materials.

Author Contributions: Conceptualization, L.K., J.E.Z. and G.D.T.; methodology, L.K., J.E.Z. and G.D.T.; experimental test, L.K. and G.D.T.; validation, L.K., J.E.Z. and G.D.T.; formal analysis, L.K., J.E.Z. and G.D.T.; investigation, L.K., J.E.Z. and G.D.T.; resources, G.D.T.; writing—original draft preparation, L.K., J.E.Z. and G.D.T.; writing—review and editing, L.K., J.E.Z. and G.D.T.; supervision, G.D.T.; project administration, G.D.T.; funding acquisition, G.D.T. All authors have read and agreed to the published version of the manuscript.

Funding: CAPES (Coordination for the Improvement of Higher Education Personnel—Brazil, funding code 001); FAPERGS (Foundation for the Support of Research in the State of Rio Grande do Sul—Brazil, process: 25/2551-0002899-0).

Data Availability Statement: The raw data supporting the conclusions of this article will be made available by the authors on request.

Acknowledgments: The author G.D. Telli thanks FAPERGS for financial support (Process: 25/2551-0002899-0). L.K. thanks CAPES for the financial support (Finance Code 001).

Conflicts of Interest: The authors declare no conflicts of interest. The funders had no role in the design of the study; in the collection, analyses, or interpretation of data; in the writing of the manuscript; or in the decision to publish the results.

Abbreviations

The following abbreviations are used in this manuscript:

BF	Basalt fiber
BFRC	Basalt fiber-reinforced concrete
BFRCT	Treated basalt fiber-reinforced concrete
BFRCT-NS	Treated basalt fiber-reinforced concrete with nanosilica
SEM	Scanning electron microscopy
NS	Nanosilica
ITZ	Interfacial transition zone

References

1. Sangoju, B.; Gopal, R.; Bhajantri, H.B. A Review on Performance-based Specifications toward Concrete Durability. *Struct. Concr.* **2021**, *22*, 2526–2538. [CrossRef]
2. Li, Z.; Ma, J.; Ma, H.; Xu, X. Properties and Applications of Basalt Fiber and Its Composites. In *Proceedings of the IOP Conference Series: Earth and Environmental Science*; Institute of Physics Publishing: Bristol, UK, 2018; Volume 186.
3. Shajidha, H.; Mortula, M.M. Sustainable Waste Management in the Construction Industry. *Front. Sustain. Cities* **2025**, *7*, 1582239. [CrossRef]
4. Teng, T.; Yang, S.; Zhao, Y.; Cui, L.; Zhang, J. Quantitative Determination of CH_4 Production and CO_2 Storage in Coal Mine Goaf: A CO_2-ECBM Recovery Model That Considers Zonal Permeability. *Green Smart Min. Eng.* **2025**, *2*, 98–108. [CrossRef]
5. Bahmani, H.; Mostafaei, H. Sustainable High-Performance Concrete: Harnessing Recycled Rubber and Slag for Strength and Eco-Friendliness. *Sci. Rep.* **2026**, *16*, 7376. [CrossRef] [PubMed]
6. Al-Rousan, E.T.; Khalid, H.R.; Rahman, M.K. Fresh, Mechanical, and Durability Properties of Basalt Fiber-Reinforced Concrete (BFRC): A Review. *Dev. Built Environ.* **2023**, *14*, 100155. [CrossRef]
7. Lee, M.-G.; Wang, W.-C.; Wang, Y.-C.; Hsieh, Y.-C.; Lin, Y.-C. Mechanical Properties of High-Strength Pervious Concrete with Steel Fiber or Glass Fiber. *Buildings* **2022**, *12*, 620. [CrossRef]
8. Raza, S.S.; Qureshi, L.A.; Ali, B.; Raza, A.; Khan, M.M. Effect of Different Fibers (Steel Fibers, Glass Fibers, and Carbon Fibers) on Mechanical Properties of Reactive Powder Concrete. *Struct. Concr.* **2021**, *22*, 334–346. [CrossRef]

9. Nassani, D.E. Experimental and Analytical Study of the Mechanical and Flexural Behavior of Hybrid Fiber Concretes. *Structures* **2020**, *28*, 1746–1755. [CrossRef]
10. Bernat, A.M.; Spinella, N.; Recupero, A.; Cladera, A. Mechanical Model for the Shear Strength of Steel Fiber Reinforced Concrete (SFRC) Beams without Stirrups. *Mater. Struct.* **2020**, *53*, 28. [CrossRef]
11. Blazy, J.; Blazy, R.; Drobiec, Ł. Glass Fiber Reinforced Concrete as a Durable and Enhanced Material for Structural and Architectural Elements in Smart City—A Review. *Materials* **2022**, *15*, 2754. [CrossRef]
12. Park, J.K.; Ngo, T.T.; Kim, D.J. Interfacial Bond Characteristics of Steel Fibers Embedded in Cementitious Composites at High Rates. *Cem. Concr. Res.* **2019**, *123*, 105802. [CrossRef]
13. Yonggui, W.; Shuaipeng, L.; Hughes, P.; Yuhui, F. Mechanical Properties and Microstructure of Basalt Fibre and Nano-Silica Reinforced Recycled Concrete after Exposure to Elevated Temperatures. *Constr. Build. Mater.* **2020**, *247*, 118561. [CrossRef]
14. Farghal, H.H.; Madkour, T.M. Basalt Fiber Composites: Structure, Properties, Sustainability, and Life Cycle Analysis. *J. Compos. Sci.* **2026**, *10*, 253. [CrossRef]
15. AL-Kharabsheh, B.N.; Arbili, M.M.; Majdi, A.; Alogla, S.M.; Hakamy, A.; Ahmad, J.; Deifalla, A.F. Basalt Fibers Reinforced Concrete: Strength and Failure Modes. *Materials* **2022**, *15*, 7350. [CrossRef] [PubMed]
16. Al-Kharabsheh, B.N.; Arbili, M.M.; Majdi, A.; Alogla, S.M.; Hakamy, A.; Ahmad, J.; Deifalla, A.F. Basalt Fiber Reinforced Concrete: A Compressive Review on Durability Aspects. *Materials* **2023**, *16*, 429. [CrossRef]
17. Algin, Z.; Ozen, M. The Properties of Chopped Basalt Fibre Reinforced Self-Compacting Concrete. *Constr. Build. Mater.* **2018**, *186*, 678–685. [CrossRef]
18. John, V.J.; Dharmar, B. Influence of Basalt Fibers on the Mechanical Behavior of Concrete—A Review. *Struct. Concr.* **2021**, *22*, 491–502. [CrossRef]
19. Xu, J.; Kang, A.; Wu, Z.; Xiao, P.; Gong, Y. Effect of High-Calcium Basalt Fiber on the Workability, Mechanical Properties and Microstructure of Slag-Fly Ash Geopolymer Grouting Material. *Constr. Build. Mater.* **2021**, *302*, 124089. [CrossRef]
20. Vatin, N.I.; Hematibahar, M.; Gebre, T.H. Impact of Basalt Fiber Reinforced Concrete in Protected Buildings: A Review. *Front. Built Environ.* **2024**, *10*, 1407327. [CrossRef]
21. Zhou, H.; Jia, B.; Huang, H.; Mou, Y. Experimental Study on Basic Mechanical Properties of Basalt Fiber Reinforced Concrete. *Materials* **2020**, *13*, 1362. [CrossRef]
22. Ja'e, I.A.; bin Raja Sazrin, R.A.N.; Syamsir, A.; Bheel, N.; Amaechi, C.V.; Min, T.H.; Anggraini, V. Optimisation of Mechanical Properties and Impact Resistance of Basalt Fibre Reinforced Concrete Containing Silica Fume: Experimental and Response Surface Assessment. *Dev. Built Environ.* **2024**, *17*, 100368. [CrossRef]
23. Ögüt, R.; Demir, A. The Effect of the Basalt Fiber on Mechanical Properties and Corrosion Durability in Concrete. *Arab. J. Sci. Eng.* **2023**, *48*, 5097–5114. [CrossRef]
24. Branston, J.; Das, S.; Kenno, S.Y.; Taylor, C. Mechanical Behaviour of Basalt Fibre Reinforced Concrete. *Constr. Build. Mater.* **2016**, *124*, 878–886. [CrossRef]
25. Liu, X.; Yang, R.; Wang, J.; Liu, Y.; Fan, Y.; He, Y.; Oterkus, E.; He, X. Atomistic Insights into the Superior Interfacial Mechanics of Basalt Fiber–Reinforced Cementitious Nanocomposite. *J. Am. Ceram. Soc.* **2026**, *109*, e70349. [CrossRef]
26. Li, L.; Zhang, L.; Zhang, Y.; Li, F. Influence of In-Situ-Grown Nano-SiO_2/Silane Coupling Agent on the Flexural Performance of Basalt Fiber-Reinforced Cementitious Composites. *J. Adhes. Sci. Technol.* **2026**, *40*, 1724–1742. [CrossRef]
27. Iorio, M.; Santarelli, M.L.; González-Gaitano, G.; González-Benito, J. Surface Modification and Characterization of Basalt Fibers as Potential Reinforcement of Concretes. *Appl. Surf. Sci.* **2018**, *427*, 1248–1256. [CrossRef]
28. Manikandan, V.; Jappes, J.T.W.; Kumar, S.M.S.; Amuthakkannan, P. Investigation of the Effect of Surface Modifications on the Mechanical Properties of Basalt Fibre Reinforced Polymer Composites. *Compos. Part B Eng.* **2012**, *43*, 812–818. [CrossRef]
29. Afroz, M.; Patnaikuni, I.; Venkatesan, S. Chemical Durability and Performance of Modified Basalt Fiber in Concrete Medium. *Constr. Build. Mater.* **2017**, *154*, 191–203. [CrossRef]
30. Deng, Y.G.; Zhao, B.J.; Dai, T.T.; Li, G.Q.; Li, Y. Study on the Dispersibility of Modified Basalt Fiber and Its Influence on the Mechanical Properties of Concrete. *Constr. Build. Mater.* **2022**, *350*, 128839. [CrossRef]
31. Sanchez, F.; Sobolev, K. Nanotechnology in Concrete—A Review. *Constr. Build. Mater.* **2010**, *24*, 2060–2071. [CrossRef]
32. Pacheco-Torgal, F.; Jalali, S. Nanotechnology: Advantages and Drawbacks in the Field of Construction and Building Materials. *Constr. Build. Mater.* **2011**, *25*, 582–590. [CrossRef]
33. Xie, L.; Sun, X.; Yu, Z.; Lian, H.; He, H.; Wang, L.; Zhang, Z.; Xu, X. Effects of Nano-Silica on Fracture Properties and Mechanism Analysis of Basalt Fiber Reinforced Concrete. *Constr. Build. Mater.* **2024**, *439*, 137375. [CrossRef]
34. Shahbazpanahi, S.; Tajara, M.K.; Faraj, R.H.; Mosavi, A. Studying the C–H Crystals and Mechanical Properties of Sustainable Concrete Containing Recycled Coarse Aggregate with Used Nano-Silica. *Crystals* **2021**, *11*, 122. [CrossRef]
35. Yonggui, W.; Jiangjiang, W.; Juan, Z. Study on the Mechanical Properties and Microstructure of Recycled Concrete Reinforced with Basalt Fibers and Nano-Silica in Early Low-Temperature Environments. *Nanotechnol. Rev.* **2024**, *13*, 20230185. [CrossRef]

36. Wang, Y.; Zhang, X.; Fang, J.; Wang, X. Mechanical Properties of Recycled Concrete Reinforced by Basalt Fiber and Nano-Silica. *KSCE J. Civ. Eng.* **2022**, *26*, 3471–3485. [CrossRef]
37. Abhilash, P.P.; Nayak, D.K.; Sangoju, B.; Kumar, R.; Kumar, V. Effect of Nano-Silica in Concrete; A Review. *Constr. Build. Mater.* **2021**, *278*, 122347. [CrossRef]
38. Zhao, L.; Chen, G.; Zhang, Y.; Zhu, H.; Zhao, H.; Tang, J.; Yuan, J. Mechanical Properties of Hybrid Fibers and Nano-Silica Reinforced Concrete during Exposure to Elevated Temperatures. *Case Stud. Constr. Mater.* **2024**, *21*, e04042. [CrossRef]
39. Mukharjee, B.B.; Barai, S.V. Influence of Incorporation of Colloidal Nano-Silica on Behaviour of Concrete. *Iran. J. Sci. Technol. Trans. Civ. Eng.* **2020**, *44*, 657–668. [CrossRef]
40. Said, A.M.; Zeidan, M.S.; Bassuoni, M.T.; Tian, Y. Properties of Concrete Incorporating Nano-Silica. *Constr. Build. Mater.* **2012**, *36*, 838–844. [CrossRef]
41. Priya, P.K.; Vanitha, S. Effect of Nano Silica on the Properties of Concrete and Mortar—A State of Art. *Int. Rev. Appl. Sci. Eng.* **2021**, *13*, 70–79. [CrossRef]
42. Yu, H.; Meng, T.; Zhao, Y.; Liao, J.; Ying, K. Effects of Basalt Fiber Powder on Mechanical Properties and Microstructure of Concrete. *Case Stud. Constr. Mater.* **2022**, *17*, e01286. [CrossRef]
43. Zhu, C.; Li, D.; Zhang, S.; Jiao, H.; Guo, J.; Chen, X. Optimal Mix Ratio and Numerical Simulation Study of Concrete Modified by Nano-Silica Synergistically Reinforced with Basalt Fibers. *Polym. Test.* **2025**, *150*, 108913. [CrossRef]
44. Mukharjee, B.B.; Barai, S.V. Influence of Nano-Silica on the Properties of Recycled Aggregate Concrete. *Constr. Build. Mater.* **2014**, *55*, 29–37. [CrossRef]
45. Chen, W.; Chen, Y. Effect of Mixed Basalt Fibers and Nano-Silica on Mechanical Properties and Microstructure of Recycled Aggregate Concrete. *AIP Adv.* **2024**, *14*, 025219. [CrossRef]
46. Wang, Y.; Cheng, J.; Wang, J. Flexural Performance of Recycled Concrete Beam Reinforced with Modified Basalt Fiber and Nano-Silica. *Case Stud. Constr. Mater.* **2023**, *18*, e02022. [CrossRef]
47. Deng, Z.; Huang, H.; Ye, B.; Xiang, P.; Li, C. Mechanical Performance of RAC under True-Triaxial Compression after High Temperatures. *J. Mater. Civ. Eng.* **2020**, *32*, 04020194. [CrossRef]
48. Lin, H.; Jiang, Y.; Li, S.; Li, W.; Zhu, D.; Chen, J.; Teng, T.; Xue, Y.; Cao, Z. In Situ Study on High-Temperature Performance and Structural Deterioration Mechanism of Concrete. *Processes* **2026**, *14*, 1753. [CrossRef]
49. Pehlivan, A.O. Effect of Nanosilica Addition on the Mechanical Properties of Cement Mortars with Basalt Fibers with or without Silica Fume. *J. Sustain. Constr. Mater. Technol.* **2022**, *7*, 17–23. [CrossRef]
50. Sharaky, I.A.; Megahed, F.A.; Seleem, M.H.; Badawy, A.M. The Influence of Silica Fume, Nano Silica and Mixing Method on the Strength and Durability of Concrete. *SN Appl. Sci.* **2019**, *1*, 575. [CrossRef]
51. *NBR 16697*; Portland Cement—Requirements. ABNT—Associação Brasileira de Normas Técnicas: São Paulo, Brazil, 2018.
52. *NBR 5738*; Concrete—Procedure for Casting and Curing of Specimens. ABNT—Associação Brasileira de Normas Técnicas: São Paulo, Brazil, 2015.
53. *ABNT NBR 5739*; Concrete—Compression Test of Cylindrical Specimens. ABNT—Associação Brasileira de Normas Técnicas: São Paulo, Brazil, 2018.
54. Cecconello, V.; Poletto, M. Assessment of Graphene Oxide Coated Polyester Fiber Reinforced Cementitious Composites. *J. Mater. Res. Technol.* **2023**, *27*, 8216–8227. [CrossRef]
55. *NBR 16889*; Fresh Concrete—Slump Test. ABNT—Associação Brasileira de Normas Técnicas: São Paulo, Brazil, 2020.
56. *NBR 12142*; Concrete—Determination of Tension Strength in Flexure of Prismatic Specimens. ABNT—Associação Brasileira de Normas Técnicas: São Paulo, Brazil, 2010.
57. *NBR 9779*; Mortar and Hardened Concrete—Determination of Water Absorption by Capillarity. ABNT—Associação Brasileira de Normas Técnicas: São Paulo, Brazil, 2012.
58. Jiang, C.; Fan, K.; Wu, F.; Chen, D. Experimental Study on the Mechanical Properties and Microstructure of Chopped Basalt Fibre Reinforced Concrete. *Mater. Des.* **2014**, *58*, 187–193. [CrossRef]
59. Katkhuda, H.; Shatarat, N. Improving the Mechanical Properties of Recycled Concrete Aggregate Using Chopped Basalt Fibers and Acid Treatment. *Constr. Build. Mater.* **2017**, *140*, 328–335. [CrossRef]
60. Wang, Y.; Hughes, P.; Niu, H.; Fan, Y. A New Method to Improve the Properties of Recycled Aggregate Concrete: Composite Addition of Basalt Fiber and Nano-Silica. *J. Clean. Prod.* **2019**, *236*, 117602. [CrossRef]
61. Zheng, Y.; Zhuo, J.; Zhang, P. A Review on Durability of Nano-SiO_2 and Basalt Fiber Modified Recycled Aggregate Concrete. *Constr. Build. Mater.* **2021**, *304*, 124659. [CrossRef]
62. Niu, D.; Su, L.; Luo, Y.; Huang, D.; Luo, D. Experimental Study on Mechanical Properties and Durability of Basalt Fiber Reinforced Coral Aggregate Concrete. *Constr. Build. Mater.* **2020**, *237*, 117628. [CrossRef]
63. Abna, A.; Mazloom, M. Flexural Properties of Fiber Reinforced Concrete Containing Silica Fume and Nano-Silica. *Mater. Lett.* **2022**, *316*, 132003. [CrossRef]

64. Ravel, R.; Pucci, M.F.; Liotier, P.J. Influence of the Surface Energy of a Basalt Fiber on Capillary Wicking and In-Plane Permeability of Reinforcements. *Compos. Part A Appl. Sci. Manuf.* **2024**, *187*, 108496. [CrossRef]
65. Qin, S.; Wu, L. Study on Mechanical Properties and Mechanism of New Basalt Fiber Reinforced Concrete. *Case Stud. Constr. Mater.* **2025**, *22*, e04290. [CrossRef]
66. Shi, W.; Guo, Y.; Liu, Y.; Wang, W.; Duan, P.; Bian, H.; Chen, J. Impact of Basalt Fiber on the Fracture Properties of Recycled Aggregate Concrete. *Constr. Build. Mater.* **2024**, *418*, 135363. [CrossRef]

Disclaimer/Publisher's Note: The statements, opinions and data contained in all publications are solely those of the individual author(s) and contributor(s) and not of MDPI and/or the editor(s). MDPI and/or the editor(s) disclaim responsibility for any injury to people or property resulting from any ideas, methods, instructions or products referred to in the content.